J. Physiol. (1973), **228**, *pp.* 459–497
With 14 *text-figures*
Printed in Great Britain

THE ROLE OF CALCIUM IN DEPOLARIZATION–SECRETION COUPLING AT THE MOTOR NERVE TERMINAL

BY J. D. COOKE,* K. OKAMOTO† AND D. M. J. QUASTEL‡

From the Department of Physiology and Biophysics, Dalhousie University, Halifax, N.S. Canada and Department of Pharmacology, University of British Columbia, Vancouver 8, B.C. Canada

(*Received 3 July 1972*)

SUMMARY

1. The relation between m.e.p.p. frequency (F) and [Ca] was studied at the mouse neuromuscular junction, at varied concentrations of K^+ and at nerve terminals depolarized by focal depolarization.

2. Under all conditions the relation between log F and log [Ca] was sigmoid, with a maximum slope that increased with depolarization or raised [K^+]. In addition, depolarization or raised K^+ caused a progressive shift of the sigmoid curve upward and to the left (to reduced log [Ca]) and increased the range over which log F could be altered by [Ca].

3. Reduction of osmotic pressure changed the relation between log F and log [Ca] in the same way as increase of depolarization, while increase of osmotic pressure did the opposite.

4. Raised [Mg] acted in two ways: (*a*) to shift the curve of log F *vs.* log [Ca] to the right and (*b*) to reduce maximum Δ log F/Δ log [Ca] without altering the range of log F sensitive to [Ca].

5. The relation between log quantal content of e.p.p.s and log [Ca] was similar to that between log m.e.p.p. frequency and log [Ca].

6. Individual nerve terminals varied in both Ca-dependent and Ca-independent fractions of log F; a large Ca-independent portion appears to be associated with a low Ca-dependent portion and vice versa. With large prolonged depolarization the Ca-independent portion was increased, apparently at the expense of the Ca-dependent portion.

7. The results of all experiments were summarized in terms of parameters found by fitting the observed log release $-$log [Ca] curves to two

* Present address: Department of Physiology, University of Western Ontario, London, Ontario.

† Present address: Kinsmen Laboratory of Neurological Research, Department of Psychiatry, University of British Columbia.

‡ Present address: Department of Pharmacology, University of British Columbia.

theoretical equations, each derived on the basis of a model: (*a*) all-or-nothing activation of release probability by Ca-complex(es) and (*b*) graded activation of release probability by Ca complex(es).

8. On the basis of the all-or-nothing model, from which follows a linear relation between F and amounts of Ca complex(es), the number of Ca^{2+} atoms that 'cooperate' to mediate release appeared to increase progressively with presynaptic depolarization, to a value of 4 or more with a presynaptic action potential.

9. On the basis of the graded activation model, which predicts an exponential relation between F and amount of Ca complex, the number of Ca^{2+} atoms that combine with Ca receptor appears to be independent of presynaptic depolarization.

10. Various models which could account for the data are discussed. It was concluded that all the data are consistent with a model in which:

(i) quantal release probability is continuously graded with the amount of a simple Ca complex (CaX) inside the nerve terminal.

(ii) Ca entry is governed by presynaptic membrane potential (increasing exponentially with depolarization) and by the amount of a Ca complex (Ca_2Y) on or in the membrane.

(iii) Mg^{2+} competes with Ca^{2+} at both receptors, X and Y.

(iv) The internal Ca receptor X is also increased by presynaptic depolarization.

INTRODUCTION

It is now well established that the quantal release of transmitter at the vertebrate neuromuscular junction, in response to motor nerve stimulation, is dependent upon and graded with the concentration of calcium ions in the bathing medium (Feng, 1936; del Castillo & Stark, 1952; del Castillo & Engbaek, 1954; Liley, 1956; Jenkinson, 1957; see review by Rubin, 1970). At the neuromuscular junction, as at the giant synapse of *Loligo*, the Ca^{2+} dependence of transmitter release is not secondary to any effect of Ca^{2+} on the presynaptic action potential (Katz & Miledi, 1965; Miledi & Slater, 1966; Katz & Miledi, 1970).

The relation between end-plate potential (e.p.p.) amplitude in the frog, and [Ca] and [Mg] was studied by Jenkinson (1957), who found the interaction of these ions to be compatible with competition of Mg^{2+} for a Ca receptor ('X') the facilitatory effect of Ca^{2+} being mediated by the complex, CaX (cf. del Castillo & Katz, 1954). E.p.p. amplitude was proportional to about the fourth power of [Ca], when [Ca] was low and/or [Mg] raised. This result was interpreted by Dodge & Rahamimoff (1967) as indicating a constant stoichiometric relation between transmitter release and Ca, four Ca^{2+} atoms being required for release of each quantum

of transmitter. However, at the rat neuromuscular junction (Hubbard, Jones & Landau, 1968*b*), as at the squid giant synapse (Katz & Miledi, 1970), the limiting slope of log transmitter release *vs.* log [Ca] was about 2·7, rather than 4; and at the rat neuromuscular junction, depolarized by 15 mM-K^+, this slope appeared to be close to unity (Gage & Quastel, 1966). Spontaneous frequency of miniature end-plate potentials (m.e.p.p.s) is even less steeply graded with [Ca] (frog: Fatt & Katz, 1952; del Castillo & Katz, 1954; rat: Hubbard, 1961; Elmqvist & Feldman, 1965; Hubbard, Jones & Landau, 1968*a*).

The present experiments were designed to explore the relation between [Ca] and transmitter release (m.e.p.p. frequency or quantal content of e.p.p.s) under several different conditions: (*a*) varied [K^+], (*b*) presynaptic depolarization by current applied focally to the end-plate and (*c*) nerve stimulation. The results show sigmoid curves relating the logarithm of release rate to log [Ca], with maximal slopes that vary with nerve terminal depolarization and other factors. These data are consistent with a model in which Ca^{2+}-sensitive depolarization evoked release is always mediated by the same simple Ca complex (CaX) located inside the nerve terminal, the logarithm of release rate being linearly related to the quantity of CaX present.

THEORY

All-or-nothing activation – 'Linear' model

The equations derived by Dodge & Rahamimoff (1967) and by Hubbard *et al.* (1968*b*) rest on the assumption that activation of release of a quantum of transmitter, by an 'activator' (e.g. a calcium complex) is all-or-nothing in character, i.e. (*a*) the presence of one or a certain fixed number of activating particles raises probability of release from an infinitesimal or zero value to a finite value and (*b*) only one kind of activator (e.g. 'X', CaX, Ca_3X, Hubbard *et al.* 1968*b*, or Ca_4X or four CaX's, Dodge & Rahamimoff (1967)) acts on any one quantum. On these assumptions, one can write generally,

$$F = a_1[A_1]+a_2[A_2]+\ldots+a_n[A_n]+\ldots \tag{1.1}$$

where F is m.e.p.p. frequency (or quantal content of e.p.p.), each $[A_k]$ is the concentration of a particular activator, and each a_k is a weighting factor reflecting the relative 'intrinsic activity' of each activator. If we consider any or all of the $[A]$'s to represent, instead of concentration of a substance in solution, the density of certain molecular configurations at critical sites, the same result applies.

Grouping each $a_k[A_k]$ into two groups, Ca^{2+}-independent and Ca^{2+}-dependent we obtain

$$F = a_0+a_1\phi([\mathrm{Ca}]) \tag{1.2}$$

where a_0 and a_1 are constants (with respect to [Ca]), and $\phi([\mathrm{Ca}])$ is an unknown function of [Ca]. Taking logarithms, and differentiating with respect to log [Ca],

$$\frac{d\log F}{d\log[\mathrm{Ca}]} = \frac{d\log\phi}{d\log[\mathrm{Ca}]}\cdot\frac{1}{1+a_0/a_1\phi} = \frac{d\log\phi}{d\log[\mathrm{Ca}]}\cdot(1-a_0/F). \tag{1.3}$$

Thus, when $a_0/a_1\phi$ is negligible, the slope $\mathrm{d}\log F/\mathrm{d}\log[\mathrm{Ca}]$ is equal to $\mathrm{d}\log\phi/\mathrm{d}\log[\mathrm{Ca}]$. Hence the result of Dodge & Rahamimoff (1967), that the maximum value of $\mathrm{d}\log F/\mathrm{d}\log[\mathrm{Ca}]$ gives a minimum value for the number of Ca^{2+} atoms which 'co-operate' for release of a quantum. For example, if Ca_nX is the Ca complex that mediates release, and the intermediate species $CaX \ldots Ca_{n-1}X$ exist to a negligible extent, we can write

$$\phi = \frac{X_t}{1+(K/[\mathrm{Ca}])^n} \tag{1.4}$$

where X_t is total Ca receptor available and K the geometric mean of the dissociation constants of the various Ca complexes. Taking logarithms and differentiating,

$$\frac{\mathrm{d}\log\phi}{\mathrm{d}\log[\mathrm{Ca}]} = \frac{n}{1+([\mathrm{Ca}]/K)^n}.$$

Thus,

$$\frac{\mathrm{d}\log F}{\mathrm{d}\log[\mathrm{Ca}]} = \frac{n}{1+([\mathrm{Ca}]/K)^n}(1-a_0/F).$$

The slope $\mathrm{d}\log F/\mathrm{d}\log[\mathrm{Ca}]$ has a maximum value always less than the maximum number, n, of Ca^{2+} atoms involved in the activating complex. It should be noted that this slope may have a maximum value considerably less than n, if a_0 is not small with respect to $a_1\phi$ when $[\mathrm{Ca}] \ll K$. Moreover, if the intermediate species (CaX, Ca_2X, etc.) do exist, this will further reduce the maximum value of $\mathrm{d}\log\phi/\mathrm{d}\log[\mathrm{Ca}]$. Thus, existing data that show maximum slopes $\mathrm{d}\log F/\mathrm{d}\log[\mathrm{Ca}]$ considerably less than 4 (see Introduction) do not necessarily exclude the generality of the 'four-Ca' model of Dodge & Rahamimoff (1967).

Continuously graded activation – 'log' model

A second model, or set of models, is generated if the all-or-nothing assumption is discarded. Let us assume, instead, that each atom or molecule of a strategically located 'activator' acts, in one way or another, to reduce an energy barrier that normally limits release of a quantum of transmitter. As a result the probability of release (in any arbitrarily small time period), which was R in the absence of activator, becomes rR, where r is greater than 1. Now, let us suppose that if there is a second particle of activator, located close by, this will further reduce the energy barrier, and, moreover, that a third and a fourth, etc. will do likewise. A simple expression results if we make two assumptions: (*a*) that the probability that a particle be present is independent of how many others are present and (*b*) that the multiplication of release probability by each is independent of how many activator particles are present. If the multiplication factor is, on average, r, for each stepwise reduction of the energy barrier, the probability of release when n particles are present will be r^nR. The mean frequency of quantal release will be proportional to the sum, over-all values of n, of the joint probability that there be n particles, and the corresponding release probability, r^nR. From assumption (*a*), the distribution of numbers of particles in space or area is random, i.e. follows Poisson's distribution, hence,

$$\begin{aligned} F &= c\sum_{n=0}^{\infty} Rr^n\lambda^n\exp(-\lambda)/n! \\ &= cR\exp[\lambda(r-1)] \\ \log F &= \log cR+\lambda(r-1), \end{aligned}$$

where λ is the mean number of activating particles per critical area or volume, and c is a constant which is governed by how many quanta are available for release.

Generalizing to a variety of activators, each acting independently to reduce the energy barrier (or a single activator generated by various stimuli), one obtains

$$\log F = a_0 + a_1[A_1] + a_2[A_2] + \ldots + a_n[A_n] + \ldots \quad (2.1)$$

where a_0 is $\log cR$ and each $a_k[A_k]$ (corresponding to $\lambda_k(r_k - 1)$ as before) represents the product of concentration (or density) of activator and a weighting factor. This equation is of the form which fits the action of certain drugs, e.g. ethanol, to multiply spontaneous and depolarization-Ca-evoked m.e.p.p. frequency to the same extent (Quastel, Hackett & Cooke, 1971).

As before, we group terms which are Ca-dependent and Ca-independent, and redefine constants, to obtain

$$\log F = a_0 + a_1\phi(\mathrm{Ca}) \quad (2.2)$$

and differentiating,

$$\frac{d\log F}{d\log[\mathrm{Ca}]} = a_1\frac{d\phi}{d\log[\mathrm{Ca}]}. \quad (2.3)$$

This result is very different from that of eqn. (1.3), since the maximum slope $d\log F/d\log[\mathrm{Ca}]$ is now not at all an index of the maximum number of Ca^{2+} atoms involved in an activating Ca complex. For example, if, as previously (eqn. (1.4)) we write,

$$\phi = X_t/(1 + (K/[\mathrm{Ca}])^n)$$

then,

$$\frac{d\phi}{d\log[\mathrm{Ca}]} = \frac{nX_t}{[1 + (K/\mathrm{Ca})^n][1 + (\mathrm{Ca}/K)^n]}$$

and,

$$\frac{d\log F}{d\log[\mathrm{Ca}]} = \frac{na_1X_t}{2 + (K/[\mathrm{Ca}])^n + ([\mathrm{Ca}]/K)^n}.$$

Thus $d\log F/d\log[\mathrm{Ca}]$ has a maximum value of $\frac{1}{4}na_1X_t$ (occurring when $K = [\mathrm{Ca}]$). If a_1X_t varies with presynaptic polarization and/or from end-plate to end-plate the maximum value of $d\log F/d\log[\mathrm{Ca}]$ will vary in proportion.

Mixed models

There is no *a priori* reason why some forms of activation should not be all-or-nothing and others graded in nature. Then, one could write

$$F = (a_1[A_1] + a_2[A_2] + \ldots).\exp(b_1[B_1] + b_2[B_2] + \ldots).$$

Such a model could accommodate both the multiplying action of ethanol and other agents, and kinetics for Ca action as proposed by Dodge & Rahamimoff (1967) or Hubbard *et al.* (1968*b*).

The Ca hypothesis

According to the 'calcium-hypothesis' of Katz & Miledi (1967, 1969, 1970), based on observations that presynaptic depolarization causes an inward current consistent with entry of Ca^{2+} or a Ca complex, transmitter release is mediated by Ca^{2+} or a Ca complex *inside* the nerve terminal. Depending on which is the case, and which set of models is taken, the Ca-hypothesis makes certain predictions.

(A) Depolarization causes entry of free Ca^{2+} and Ca complex(es) in the nerve terminal mediate release

Provided the effect of depolarization on Ca entry is independent of $[\mathrm{Ca}]_{out}$ the effect of polarization will simply be to alter the ratio of $[\mathrm{Ca}]_{in}$ to $[\mathrm{Ca}]_{out}$, i.e. it is possible to write

$$[\mathrm{Ca}]_{in} = f(V)[\mathrm{Ca}]_{out},$$
$$\log[\mathrm{Ca}]_{in} = \log f(V) + \log[\mathrm{Ca}]_{out}.$$

Thus, for *any* functional relationship between $[Ca]_{in}$ and F, a graph of F (or $\log F$) *vs.* $\log[Ca]_{out}$ will remain constant in form, only being shifted in parallel on the $\log[Ca]_{out}$ axis as $f(V)$ is altered.

(B) Depolarization causes entry of Ca^{2+} derived from a Ca-complex, or of Ca-complex(es), the form that enters itself being the activator of release:

(i) *All-or-nothing model.* If we assume that only one form of Ca-complex exists (or that all Ca-complexes are moved in proportion) and that release is simply proportional to the amount of 'activator' inside the nerve terminal, then from (1.2).

$$F = a_0 + a_1 f(V).\phi(\mathrm{Ca}). \tag{1.5}$$

As $f(V)$ becomes large, a_0 becomes relatively small, therefore $(d\log F/d\log[Ca])_{max}$ approaches n. A graph of $\log(F-a_0)$ *vs.* [Ca] or log[Ca] is simply shifted upwards as $f(V)$ increases.

(ii) *Continuously graded model.* Here we assume $\log F$ is proportional to 'activator' inside the terminal. The equation corresponding to (1.5) is,

$$\log F = a_0 + a_1 f(V).\phi[\mathrm{Ca}]. \tag{2.5}$$

Hence, the slope $d\log F/d\log[Ca]$ is continuously graded with $f(V)$. A graph of $(\log F - a_0)$ *vs.* [Ca] or log[Ca] is altered by a scaling of the ordinate.

(C) There exist various Ca complexes (e.g. CaX, Ca_2X, Ca_3X etc.) in or on the membrane and depolarization alters entry of each species, to different extents

The equations now take the form

$$F \text{ (or } \log F) = \frac{a_0 + a_1 f_1(V)[\mathrm{Ca}] + a_2 f_2(V)[\mathrm{Ca}]^2 + a_3 f_3(V)[\mathrm{Ca}]^3 + \ldots}{1 + b_1[\mathrm{Ca}] + b_2[\mathrm{Ca}]^2 + b_3[\mathrm{Ca}]^3 + \ldots} \tag{3.1}$$

In the case of the all-or-nothing model, since maximum $d\log F/d\log[Ca]$ may be at least 4, we must consider all coefficients in the above expression, at least up to those of $[Ca]^4$. Thus any curve fitting will involve at least nine parameters, with at least four of these being functions of presynaptic polarization. Given limitations of data accuracy, this model becomes essentially untestable. In the case of the model of continuously graded activation, fewer coefficients might suffice and the model become testable.

METHODS

The methods for superfusion of hemidiaphragms, *in vitro*, focal polarization of end-plates, and recording have been described elsewhere (Cooke & Quastel, 1972*a*). In preliminary experiments both rat and mouse diaphragms were used, with no apparent difference in results; all the results reported here are from mouse diaphragms. The experiments were carried out at a temperature of 28–30° C: preliminary experiments showed no obvious differences in results over a temperature range of 25–35° C.

Solutions. In preliminary experiments, the experiments reported on the time course with which m.e.p.p. frequency alters with [Ca] changes, and the experiments with end-plate potentials, standard bathing solution had the same composition as previously (Cooke & Quastel, 1972*a*). For the major series of experiments in which the relation between m.e.p.p. frequency and [Ca] was studied at various $[K^+]$, NO_3^- was substituted for Cl^-, $[Na^+]$ reduced by 30 mM, and sucrose added to bring all solutions to the same osmotic pressure as the solution containing 50 mM-K^+. Thus all 'isotonic' solutions were hyperosmolar to the same extent, equivalent to addition

of 20 mM-NaCl or KCl to standard solution. The reason for NO_3^- substitution for Cl^- was to make larger the m.e.p.p.s recorded in high K^+ solution: control experiments showed substitution of NO_3^- for Cl^- to have no discernible action on m.e.p.p. frequency, at any $[K^+]$. Reduction of $[Na^+]$ was done primarily to avoid gross hyperosmolarity in all solutions, but also had the effect of shifting curves of log m.e.p.p. frequency *vs.* log [Ca] to the left (cf. Gage & Quastel, 1966). This shift was not studied in detail.

In the Results, stated [Ca] concentrations are the amounts of Ca^{2+} added to solutions. Examination of nominally Ca^{2+}-free solutions by atomic absorption spectrophotometry showed [Ca] = 0·003 mM (range 0·0025–0·0034 mM). For all calculations this value was added to the nominal [Ca].

Counting of m.e.p.p.s. In all experiments final counts of m.e.p.p. frequencies were made from the Mingograf record. However, during experiments m.e.p.p. frequency was continuously monitored, with an accuracy which varied with noise level, m.e.p.p. size and frequency, by a PDP-12 computer, programmed to count m.e.p.p.s according to two criteria: (*a*) rate of rise, and (*b*) area over a 1 msec period. Numbers of m.e.p.p. counted were typed out, and a signal corresponding to each putative m.e.p.p. counted by the computer was recorded on the paper record. Thus, it was possible during each experiment to be sure that m.e.p.p. frequency had reached its equilibrium value before changing the superfusion to a new solution.

Measurement of quantal content. Quantal content was estimated by any of three methods, depending on its value: (1) method of failures, (2) direct method and (3) variance method (Hubbard, Llinás & Quastel, 1969). The last was used only in experiments in which D-tubocurarine was used to keep e.p.p.s subthreshold. Control experiments showed D-tubocurarine in the amounts used ($0·5–2 \times 10^{-7}$ g/ml.) to have no detectable effect on quantal content at end-plates where it was also possible to record e.p.p.s in the absence of D-tubocurarine (by using relatively high frequency stimulation). For the method of failures, the PDP-12 was programmed to count 'successes', defined as a deflexion of the record greater than a present level, in a preset period of time following nerve stimulation. When the threshold level for counting was adjusted so that no 'successes' were missed, there were occasionally false counts corresponding to recording noise. However, these false counts could always be recognized, and discarded, by examination of the Mingograf record. The 'direct' method, i.e. comparison of mean e.p.p. amplitude with m.e.p.p. amplitude, was used whenever 'failures' were fewer than about 10% of all e.p.p.s, and gave the same values for quantal content as either the method of failures or variance method, applied to the same data.

Fitting of data points to theoretical equations. To summarize the relation between m.e.p.p. frequency and [Ca], data points from each series (from individual end-plates, or 'multiple sampling') were fitted (by standard non-linear least squares methods) to two different equations:

$$(a)\ \log F = \log[\alpha + \beta\{1 + (\gamma[\mathrm{Ca}]^{-1})^{\theta}\}^{-1}]. \tag{4.1}$$

and,

$$(b)\ \log F = \alpha + \beta\{1 + (\gamma[\mathrm{Ca}]^{-1})^{\theta}\}^{-1}. \tag{4.2}$$

Each of these equations represents simplification of eqn. (3.1), with the minimal number of parameters necessary to account for the data points observed. Eqn. (*a*) was written in the logarithmic form of two reasons: (i) because the accuracy of $\log F$ rather than F was uniform and (ii) to permit the residual squares of deviations from the best-fitting theoretical curve to be directly comparable to that obtained with eqn. (4.2). Each computation was done both with θ fixed at integral values, and with θ free to vary ('float') to obtain its best-fitting value. After it was found that

the data showed systematic deviations from the symmetry demanded by both of the above equations, data series were also fitted to the equation,

$$\log F = \alpha + \beta\{1 + \gamma^2([\mathrm{Ca}]^{-2} + \epsilon[\mathrm{Ca}]^{-1})\}^{-1} \quad (4.3)$$

with ϵ fixed according to the average deviation of series done at the same magnesium concentration. This was possible because θ, by eqn. (4.2), was always close to 2. The equivalent modification to eqn. (4.1) was not attempted, after examination of data showed no fixed extra parameter could suffice; an extra free-floating variable would be necessary to summarize the data points.

In no series were the m.e.p.p. frequencies observed in '0'-Ca^{2+}, i.e. 0·1 mM-Ca^{2+}, 1 mM-MgEDTA, used in fitting series of data points to either model. These points were excluded on the following grounds: (i) there might exist a component of F (or $\log F$) constant throughout the range of [Ca]'s employed, but much reduced in very low [Ca] (cf. Cooke & Quastel, 1972*b*), and the actual treatment permitted examination of the data to see if this were the case; (ii) relative inaccuracy of determination of the very low m.e.p.p. frequencies found in '0'-Ca^{2+}, which would lead to biasing of the parameters found by least-squares fitting.

Accuracy of data. Except where m.e.p.p. frequency was extremely low, m.e.p.p. frequency estimations were made on the basis of at least one hundred (usually several hundred) m.e.p.p.s counted. From the Poisson distribution, this would lead to an accuracy of each point of $\pm 10\%$ or better, or, in terms of log m.e.p.p. frequency, an accuracy of $\pm 0{\cdot}1$ or less. Thus, after fitting data series to the equations a residual 'mean square' of 0·01 could be expected simply from inaccuracy of data. In fact, residual mean squares were consistently less than this value.

In the experiments using 'multiple sampling', m.e.p.p. frequency (or quantal content) was measured at about twenty-five end-plates. The m.e.p.p. frequencies found generally fitted well a log normal distribution (cf. Gage & Quastel, 1966): means and standard errors were calculated from individual values of $\log F$. In all cases, a sample of twenty-five end-plates yielded a standard error of $\log F$ of about 0·1. Thus the accuracy of the data points obtained by the multiple sampling method in a hemidiaphragm was equivalent to that of the data from any one end-plate.

RESULTS

Response of m.e.p.p. frequency to changes of [Ca] in preparations equilibrated in raised [K^+]

Time course of m.e.p.p. frequency changes. In diaphragms equilibrated in solution containing raised [K^+] (15 mM or greater) and 2 mM-Ca^{2+} the immediate response to reduction of [Ca] was an increase of m.e.p.p. frequency (F), and raised [Ca] caused reduction of F. These phenomena are illustrated in Fig. 1. In this sequence from an end-plate in 15 mM-K^+ it is also evident that reduction of [Ca] from 8 mM revealed that concentrations of Ca^{2+} above 2 mM have an excitatory action that normally is obscured by an inhibitory effect. The last sequence of [Ca] changes in Fig. 1 illustrates the slow fall of F to a low rate with reduction of [Ca] to a low level (0·125 mM). After equilibration in low Ca^{2+}, the response to increase of [Ca], to the original 2 mM, was an almost immediate restoration of the F characteristic of equilibration at this [Ca]. However, subsequent reduction of [Ca] was now followed by a prompt reduction of F.

In general, the time course with which F fell after reduction of [Ca] was graded with duration of exposure to raised [Ca]; F fell rapidly in low [Ca] to its equilibrium level after a brief (about 1 min) exposure to raised [Ca], but much more slowly if exposure to raised [Ca] had been continued for more than a few minutes. This behaviour suggests that there normally

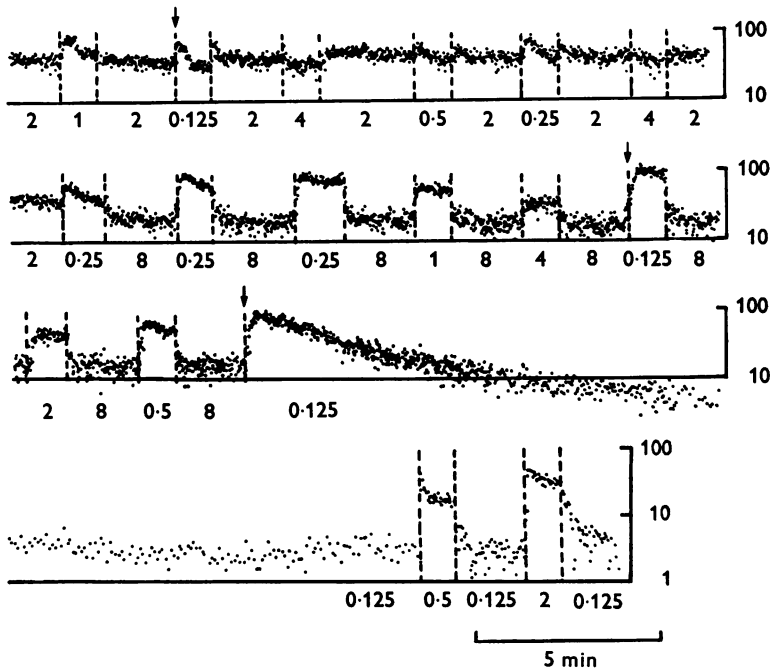

Fig. 1. Alteration of m.e.p.p. frequency by rapid changes of [Ca] at an end-plate equilibrated in 15 mM-K^+. Interrupted bars indicate change of superfusing [Ca]. Each point corresponds to number of m.e.p.p.s counted in 2 sec period, plotted semilogarithmically *vs.* time. Note the transient increase of m.e.p.p. frequency upon switching to low Ca^{2+} – the transient was higher and better sustained the higher the preceding [Ca] (compared middle sequence with top sequence). Arrows emphasize switches to 0·125 mM-Ca^{2+}. Note also, in second and third row inverse gradation of m.e.p.p. frequency with [Ca], following exposure to 8 mM-Ca^{2+}. Responses in bottom row illustrate that m.e.p.p. frequencies in 2 mM-Ca^{2+}, after 20 min in 0·125 mM-Ca^{2+}, were the same as after equilibration in 2 mM-Ca^{2+}, and frequency in 0·5 mM-Ca^{2+} was less. [Mg] was constant, 0·5 mM.

exists a store or pool of Ca^{2+} which can sustain the concentration of Ca^{2+} at the sites where [Ca] exerts its facilitating action, and therefore maintain F despite withdrawal of Ca^{2+} from the bathing solution.

In the presence of raised [Mg] the temporary maintenance of F in low

[Ca] was a much less apparent phenomenon, suggesting that Mg^{2+} may substitute for Ca^{2+} in this pool or store. Moreover, the inhibitory action of raised [Mg] on F always appeared immediately (whatever the [Ca]) without any phase of raised m.e.p.p. frequency (Fig. 2).

The mechanism of the inhibitory action of Ca^{2+} is considered in some detail in an accompanying paper (Cooke & Quastel, 1972*c*). It will suffice here to state that the inhibition appears to be exerted on a specific action of K^+ but does not imply that increase of F by raised K^+ is not primarily due to nerve terminal depolarization.

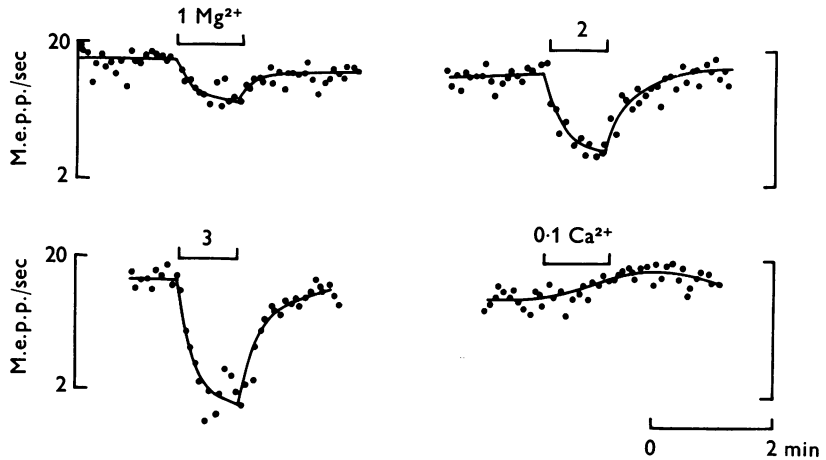

Fig. 2. Response of m.e.p.p. frequency increase of [Mg] from 0·5 mM to 1, 2, and 3 mM. Semilog plot. $[K^+]$ = 15 mM, [Ca] = 2 mM. Last sequence shows slight increase of m.e.p.p. frequency produced by reduction of [Ca] to 0·1 mM, at the same end-plate.

The rise in F that occurs in low [Ca] following equilibration in normal or high [Ca] could not be prevented by complete withdrawal of Ca^{2+} from the bathing solution. However, in solution containing a Ca^{2+}-chelator (EDTA or EGTA) even buffered, i.e. an excess of total [Mg] over [EDTA], m.e.p.p. frequencies fell sharply without the appearance of 'disinhibition' although it still required at least 5 min before F fell to its rather low equili brium level (usually between 0·1 and 1 m.e.p.p./sec).

In diaphragms equilibrated in raised $[K^+]$ and low [Ca], or after relatively brief exposure to solution with little or no Ca^{2+} and added EDTA or EGTA, subsequent increases of [Ca] resulted in fairly rapid attainment of the F characteristic of that Ca^{2+} concentration (Figs. 1, 3). The time course of the increase of F with raised [Ca] varied considerably from junction to junction. Often it was complete in less than half a minute; presumably this was at junctions very superficial in location (e.g. Fig. 1).

At all junctions the values of F achieved were independent of whether the previous bathing solution contained a very low [Ca], or a [Ca] only slightly less than the test solution. Thus, graphs of F *vs.* [Ca] were the same whether [Ca] was progressively increased, or whether a low calcium solution was used between trials.

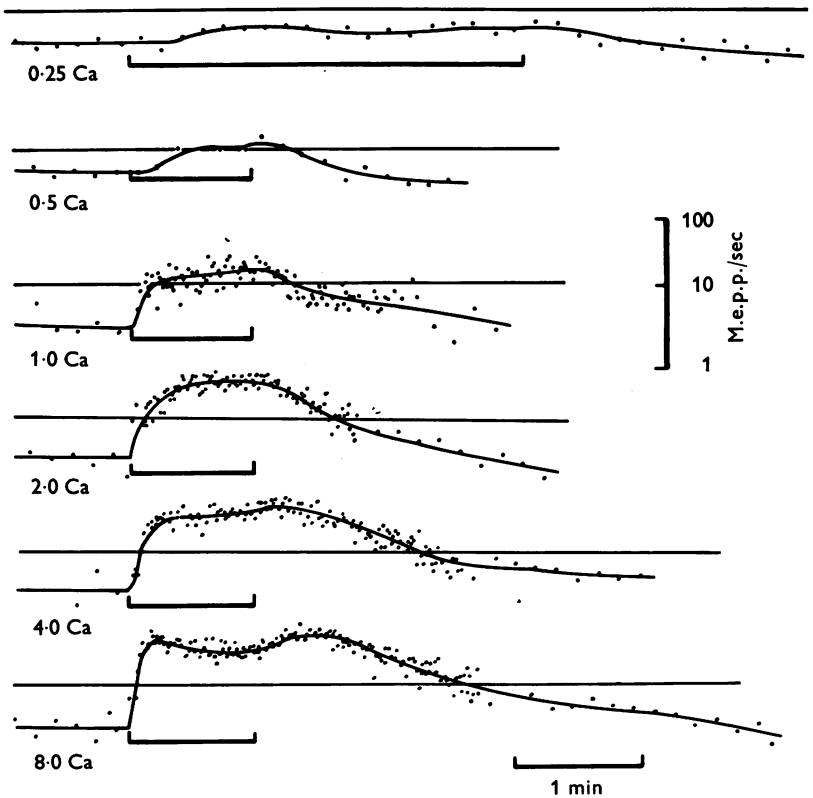

Fig. 3. Response of m.e.p.p. frequency to [Ca] increases at end-plate equilibrated in 15 mM-K^+, 0·125 mM-Ca^{2+}. Solution switched to indicated [Ca] for periods shown by horizontal bars. Note slight lag in responses and relatively slow decay of m.e.p.p. frequency upon return to 0·125 mM-Ca^{2+}. The responses to 4 and 8 mM-Ca^{2+} illustrate slightly delayed appearance of inhibitory action of Ca^{2+}, followed by 'disinhibition' on return to low [Ca]. [Mg] = 1 mM.

Relation between m.e.p.p. frequency and [Ca]. The relation between F and [Ca] at various [K^+] was determined in two ways: (*a*) at individual end-plates equilibrated in '0'-Ca^{2+} and subsequently exposed to increasing concentrations of [Ca], and (*b*) multiple sampling, to obtain estimates of mean F in a diaphragm, in each test solution. Fig. 4 shows the relation

between F and [Ca] at one end-plate in 20 mM-K^+. The graph shows the characteristic sigmoid relation between log F and log [Ca] found in all these experiments. The data from experiments using multiple sampling are shown in Fig. 5: (*a*) maximum $\Delta \log F/\Delta \log [Ca]$ increases with [K^+], at least up to 20 mM, (*b*) the range of F sensitive to [Ca] increases with [K^+], (*c*) the centre of the 'S' of the sigmoid relation is shifted to the left on the abscissa.

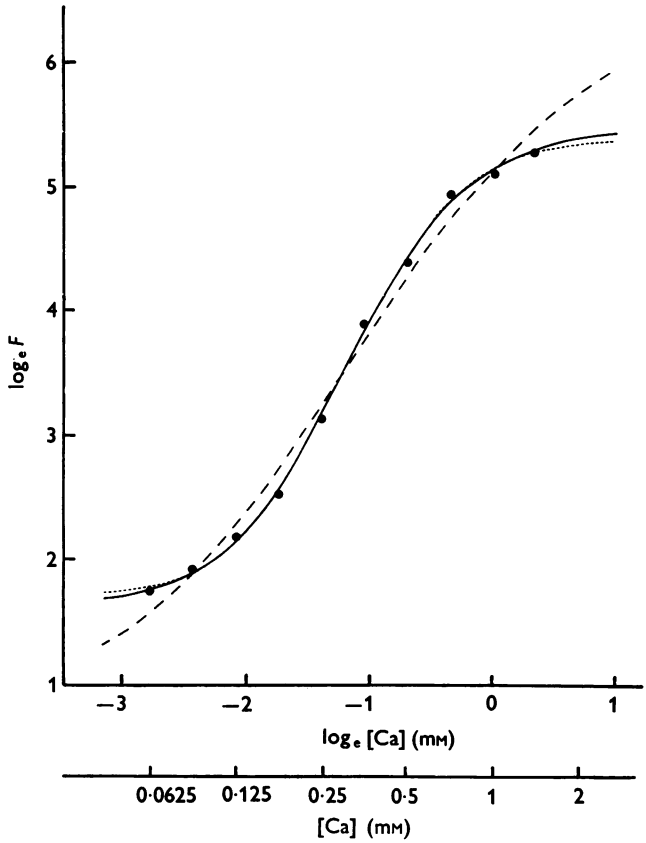

Fig. 4. Graph of log m.e.p.p./sec (log F) *vs.* log [Ca] (natural logarithms) from an end-plate equilibrated in 20 mM-K^+. Lines drawn follow the following equations:

Continuous line: $\log F = \alpha + \beta\{1 + (\gamma[Ca]^{-1})^2\}^{-1}$ $\alpha = 1{\cdot}61$, $\beta = 3{\cdot}877$, $\gamma = 0{\cdot}302$ mM.

Large dashes: $\log F = \alpha + \beta\{1 + \gamma[Ca]^{-1}\}^{-1}$ $\alpha = 0{\cdot}59$, $\beta = 5{\cdot}960$, $\gamma = 0{\cdot}308$ mM.

Small dashes: $F = \alpha + \beta\{1 + (\gamma[Ca]^{-1})^{\theta}\}^{-1}$ $\theta = 2{\cdot}67$, $\alpha = 5{\cdot}5$, $\beta = 212$, $\gamma = 0{\cdot}601$ mM.

Note first and third theoretical lines are indistinguishable except at the extremes and provide equally good fits to the data points.

In preliminary experiments it was found that the 'multiple sampling' method showed considerable variation in mean F, from one diaphragm to another in the same solution, although changes in $\log F$ with change of [K^+] and [Ca] were highly reproducible. That is, differences of F's, between two diaphragms could be accounted for by a single multiplying constant. To obtain these adjustment factors for the three diaphragms employed for the data of Fig. 5, m.e.p.p. frequencies were sampled in these diaphragms in common solutions (e.g. 15 mM-K^+, 0·5 mM-Ca^{2+}) as well as in

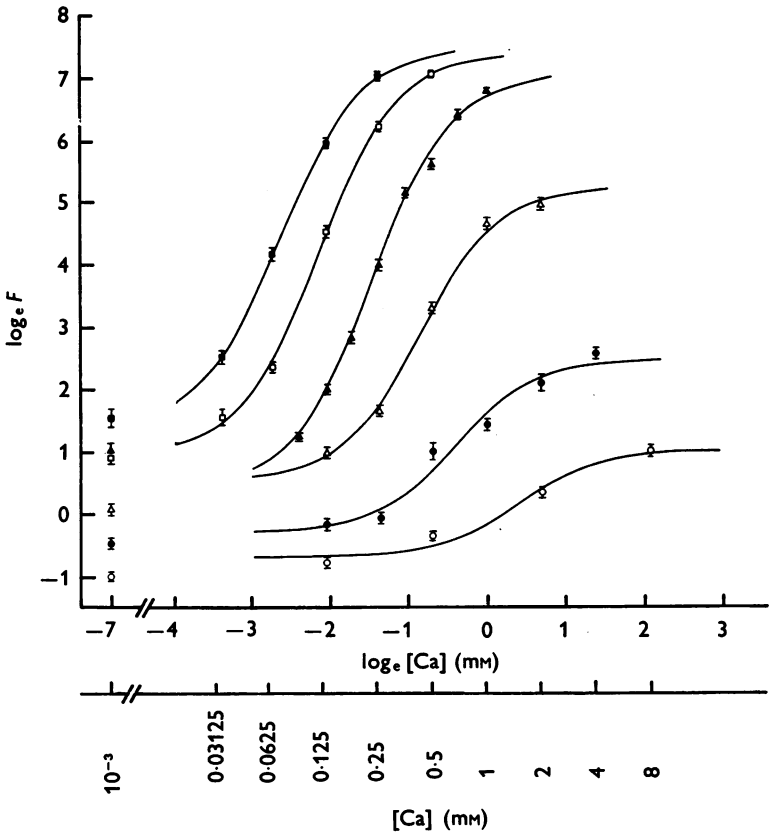

Fig. 5. Graphs of $\log F$ *vs.* $\log$ [Ca] obtained by multiple sampling of three diaphragms, in 5 mM-K^+ (○), 10 mM-K^+ (●), 15 mM-K^+ (△), 20 mM-K^+ (▲), 30 mM-K^+ (□) and 50 mM-K^+ (■). Series in 5 and 10 mM-K^+ from one diaphragm, 15, 30 and 50 mM-K^+ from another, and 20 mM-K^+ from another. All points except those for 5 and 10 mM-K^+ have been raised (see text) to adjust for variation of α between diaphragms. Lines are theoretical curves fitting eqn. (4.3).

the main series of solutions. On the basis of the differences found, all the points for 15, 30 and 50 mM-K are plotted in Fig. 5 at 1·575 $\log_e$ units above true values, and those for 20 mM-K^+ at 1·346 $\log_e$ units above true values. After this adjustment it appears that the Ca^{2+}-independent fraction of F or $\log F$ progressively increases with [K^+].

In all cases, the sigmoid curve relating $\log F$ to $\log[Ca]$ could be fitted closely, and about equally well to either of the two functions chosen (eqns. (4.1) and (4.2) in Methods). As is apparent in Fig. 4, both functions, with appropriate constants, could give virtually identical theoretical curves. In accord with the obvious increase in $\Delta \log F / \Delta \log[Ca]$ seen in Fig. 5, fitting of the data series from individual end-plates to the equation of the 'linear' model showed a progressive increase in θ (the number of Ca atoms that appear to 'co-operate' for release of each quantum of transmitter) with

TABLE 1. Estimates of 'θ' and 'γ' obtained by least-squares fitting of F *vs.* [Ca] curves to equations corresponding to 'linear' and 'log' models

		θ		γ	
$[K^+]$	n†	'linear'	'log'	'linear'	'log'
5	*	0·95	—	6·43	0·95 ± 0·23
10	*	1·51 ± 0·50	—	2·21 ± 0·24	0·68 ± 0·18
15	7	2·60 ± 0·21	1·94 ± 0·27	1·07 ± 0·16	0·45 ± 0·02
20	19	3·03 ± 0·12	1·99 ± 0·12	0·64 ± 0·05	0·28 ± 0·01
25	6	2·94 ± 0·17	1·74 ± 0·32	0·49 ± 0·07	0·19 ± 0·01
30	6	3·44 ± 0·21	1·96 ± 0·19	0·30 ± 0·02	0·13 ± 0·01
50	3	3·23 ± 0·19	1·83 ± 0·52	0·39 ± 0·21	0·10 ± 0·01

* Data from experiments using multiple sampling – one series each.
† Number of end-plates 'followed'.

increasing $[K^+]$ (Table 1). Moreover, there appeared to be significant differences of θ from one end-plate to another, at the same $[K^+]$. For example, for the data series plotted in Fig. 4 best fitting θ was 2·67, with a residual mean square (sum of squares of deviation divided by degrees of freedom) of 0·0036. With integral values of θ (2 or 3) mean squares were considerably greater (0·0127 and 0·0052 respectively). For all nineteen junctions in 20 mM-K^+, mean θ was 3·03, but fitting all the series with θ fixed at 3 (instead of 'floating') yielded a mean square of 0·0085, very significantly higher than the mean square of 0·0060 obtained with θ free to vary ($P < 0{\cdot}005$ by 'F' test, although this test is not strictly applicable for non-linear fitting a value of 'F' of 3·6, nearly double that significant at the 0·5% level, can be considered indicative).

In contrast, fitting of the data to the 'log' model yielded, for each $[K^+]$ a mean θ close to 2·0 (Table 1); rise of β with $[K^+]$ accounted entirely for increase of maximum $\Delta \log F / \Delta \log[Ca]$ (Fig. 7). Moreover, fitting *all* the data series with θ fixed at 2·0 resulted in mean squares not significantly higher than with θ free to vary (or with fitting to the 'linear' model, with θ free to vary). It should be noted, however, that θ was rather poorly defined (S.D. = 0·61) by any individual data series (from an individual end-plate or by multiple sampling).

The excellent fit of the data to eqn. (4.2) strongly suggests that log F is in general governed by the amount of a Ca complex, Ca_2X, at certain sites. However, exact correspondence to the equation could occur only if the intermediate species, CaX, existed only in negligible quantity. If the amount of this species were not negligible, a better fit would be expected with the following formula

$$\log F = \alpha + \beta\{1 + \gamma^2([Ca]^{-2} + \epsilon[Ca]^{-1})\}^{-1} \quad (4.3)$$

where ϵ depends upon the dissociation constants of the Ca complex and may or may not vary with γ, depending on the kinetic model chosen (see Discussion). The effect of ϵ on the log F *vs.* log[Ca] curve is twofold: (*a*) to reduce apparent θ when data are fitted to eqn. (4.2) and (*b*) to introduce a skewing of the curve, with $d\log F/d\log[Ca]$ falling more slowly with [Ca] higher than γ than would otherwise be the case.

By differentiating eqn. (4.2) and rearranging, one finds

$$\beta^{-1} d\log F/d\log[Ca] = \theta\{(\log F - \alpha)\beta^{-1} - (\log F - \alpha)^2 \beta^{-2}\},$$

i.e. for all data that fit eqn. (4.2) exactly, a graph of normalized slope, i.e.

$$\beta^{-1}\Delta \log F/\Delta \log[Ca],$$

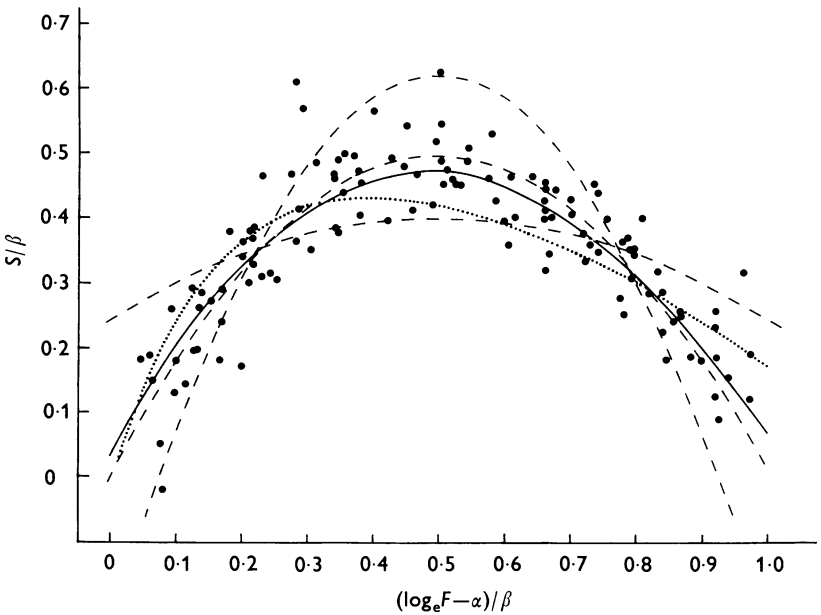

Fig. 6. Plot of $\beta^{-1}\Delta \log F/\Delta \log[Ca]$ ('$S\beta^{-1}$') *vs.* $(\log F - \alpha)\beta^{-1}$ data adjusted (see text) for inhibitory action of Ca^{2+}. Points from nineteen experiments with 'isotonic' 20 mM-K^+. Lines are theoretical curves for the following functions: continuous line: $\log F = \alpha + \beta\{1 + \gamma^2([Ca]^{-2} + [Ca]^{-1})\}^{-1}$; dashed lines: $\log F = \alpha + \beta(1 + \gamma^\theta[Ca]^{-\theta})^{-1}$ for θ = 1, 2, 3 (flattest curve is for θ = 1); dotted line: $F = \alpha + \beta\{1 + \gamma[Ca]^{-1}\}^{-\theta}$ θ = 4, β/α = 1000. Note that all but last curve are independent of parameters α, β, γ. For last function curve alters with all parameters, but always retains asymmetry and provided very poor fit. It is close to invariant for $(\log F - \alpha)\beta^{-1} > 0{\cdot}5$. All theoretical curves generated from 'dummy' data treated exactly like real data, i.e. α, β, γ found by fitting to eqn. (4.2). Note best fit with continuous line, i.e. to eqn. (4.3) with ϵ = 1.

vs. normalized m.e.p.p. frequency (i.e. $\beta^{-1}(\log F - \alpha)$) would give an invariant parabola. On this basis, a search was made for any consistent deviations of the data from eqn. (4.2), with negative results. A slightly different result emerged upon taking into account the inhibitory action of high [Ca] on m.e.p.p. frequency in raised [K^+] (Figs. 1, 3; Cooke & Quastel, 1972*c*). Although this action is not large at [Ca] < 2 mM, ignoring it could lead to spuriously low slopes of $\Delta \log F / \Delta \log [Ca]$ at the higher [Ca]'s in each series, and perhaps a spuriously good fit to the equation. From the data of Cooke & Quastel (1972*c*) Ca^{2+} inhibition appears to act on the Ca^{2+}-dependent fraction of $\log F$, and at least for [Ca] < 2 mM, is such as to divide the Ca^{2+} dependent fraction of $\log F$ by the factor $(1 + 0{\cdot}1\,[Ca])$. After the appropriate adjustments, examination of the normalized data (with re-evaluated α, β and γ) now showed significant deviations from eqn. (4.2), for the 15 mM-K^+ ($P < 0{\cdot}05$) and 20 mM-K^+ ($P < 0{\cdot}005$) series. Fig. 6 shows a plot of the points available from the 20 mM-K^+ series: $\beta^{-1}\Delta \log F / \Delta \log [Ca]$ is plotted *vs.* $(\log F - \alpha)\beta^{-1}$. The points fall less steeply with $(\log F - \alpha)\beta^{-1}$ above 0·5 than predicted by eqn. (4.2) with $\theta = 2$. This deviation is in the direction expected for appreciable ϵ in eqn. (4.3), and indicated an ϵ of about

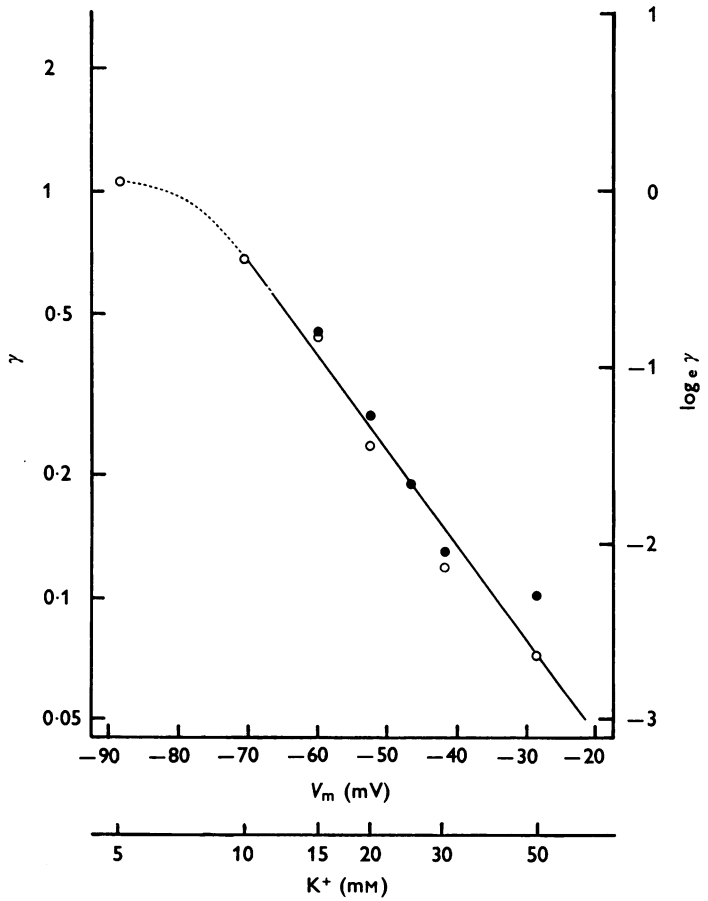

Fig. 7*A*. For legend see facing page.

1, as did also the data from the 15 mM-K^+ series. For the other series, with higher [K^+], deviations from eqn. (4.2) were not significant, but this would be expected from eqn. (4.3), with $\epsilon = 1$ and low values of γ.

Fig. 7*A* shows a semilogarithmic plot of γ (by least-squares fitting to eqn. (4.3) with $\theta = 2$, $\epsilon = 1$; values were virtually the same with $\epsilon = 0$ and θ 'floating') *vs.* nominal presynaptic membrane potential calculated by

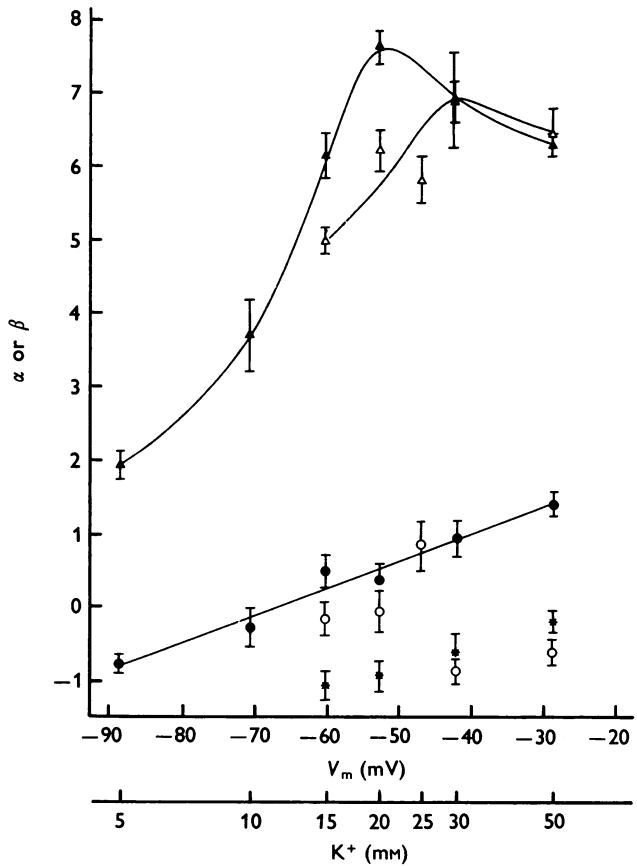

Fig. 7*B*.

Fig. 7 *A*, graph of log γ (by fitting to eqn. (4.3) with $\epsilon = 1$) *vs.* nominal membrane potential (calculated by Nernst equation). (○) γ from multiple sampling experiments (●) mean γ's from individual end-plates. The continuous line is the regression line, by least squares, for all points except that for 5 mM-K^+. Its slope is $-0{\cdot}053 \pm 0{\cdot}004$/mV.

B, graph of β and α (eqn. (4.3), with $\epsilon = 1$) *vs.* nominal membrane potential. Filled symbols, derived data from multiple sampling experiments; open symbols, derived means from individual end-plate. Circles, α; triangles, β. α's from multiple sampling experiments for 15, 20, 30 and 50 mM-K^+ are adjusted for variation between diaphragms. The corresponding unadjusted α's are also plotted (asterisks). Lines drawn by eye.

the Nernst equation. Excluding only the point of 5 mM-K^+ there is an obvious linear correlation of $\log \gamma$ with membrane potential ($r = 0{\cdot}978$). The slope of the regression line is $-0{\cdot}053 \pm 0{\cdot}004$/mV, i.e. γ^{-1} increased e-fold for each 18·9 mV increment of membrane potential. Values of γ found by fitting to the 'linear' model (eqn. (4.1)) also showed significant regression with [K^+] (Table 1).

TABLE 2. Derived data from experiments with 20 mM-K^+ and varied osmotic pressure

		Change of osmotic pressure m-osmole		
		−50	0	+50
No. of end-plates		5	7	7
A 'Linear'* model	θ	3·34 ± 0·20	2·82 ± 0·14	2·68 ± 0·14
	α	3·1 ± 0·4	4·1 ± 0·4	3·5 ± 1·3
	$\log_e \beta$	5·94 ± 0·07	5·49 ± 0·15	4·59 ± 0·22
	γ	0·41 ± 0·04	0·55 ± 0·03	0·64 ± 0·06
B 'Log' model†	α	0·66 ± 0·25	1·23 ± 0·12	0·87 ± 0·33
	β	6·27 ± 0·37	5·19 ± 0·20	4·83 ± 0·41
	γ	0·20 ± 0·02	0·27 ± 0·02	0·35 ± 0·03

* Data from each end-plate fitted to $F = \alpha + \beta\{1 + (\gamma[\mathrm{Ca}]^{-1})^{\theta}\}^{-1}$.

† Data from each end-plate fitted to $\log F = \alpha + \beta\{1 + \gamma^2([\mathrm{Ca}]^{-2} + [\mathrm{Ca}]^{-1})\}^{-1} \times \{1 + 0{\cdot}1[\mathrm{Ca}]\}^{-1}$.

In Fig. 7*B* are plotted values of α and β (eqn. (4.3), $\theta = 2$, $\epsilon = 1$) *vs.* calculated membrane potential: β evidently increases with depolarization until membrane potential is between 50 and 40 mV, but subsequently declines, and there is a suggestion of increase of α with depolarization.

Effects of altered osmotic pressure. In preliminary experiments it was noted that maximum $\Delta \log F / \Delta \log [\mathrm{Ca}]$ at any one [K^+] was markedly altered by changes in osmotic pressure: for this reason all the solutions in the above series were adjusted to the same osmotic pressure (see Methods). In the present series the response of F to [Ca] (in 20 mM-K^+) was followed at five junctions in solution which was hypotonic by 50 m-osmoles, seven in 'isotonic' solution and seven in solution made hypertonic by the further addition of 50 mM sucrose. In all cases the graphs of $\log F$ *vs.* $\log$[Ca] resembled that shown in Fig. 4, and fitting of the data to the 'log' model showed 'θ' not appreciably nor significantly different from 2. Table 2 shows the data derived from these series: (*a*) by fitting of the data of each series to the 'linear' model and, (*b*) by fitting to the 'log' model, with $\theta = 2$ and $\epsilon = 1$, and adjustment for Ca^{2+} inhibition in the same way as previously. Evidently, hypo-osmolarity acted to change the parameters in much the same way as an increase of [K^+] while hyperosmolarity did the reverse. With the 'linear' model (Table 2*A*), there appeared to be a

significant alteration by osmotic pressure of θ as well as of β and γ (correlation of each parameter is significant at 1 % level or better). Thus, according to the 'linear' model, alteration of osmotic pressure acts like alteration of $[K^+]$, to change the number of Ca^{2+} atoms that 'co-operate' for release of each quantum of transmitter.

Magnesium. Jenkinson (1957) and Dodge & Rahamimoff (1967) have presented data consistent with the hypothesis that the inhibitory action of Mg^{2+} on transmitter release (e.p.p.s.) is via simple competition with Ca^{2+},

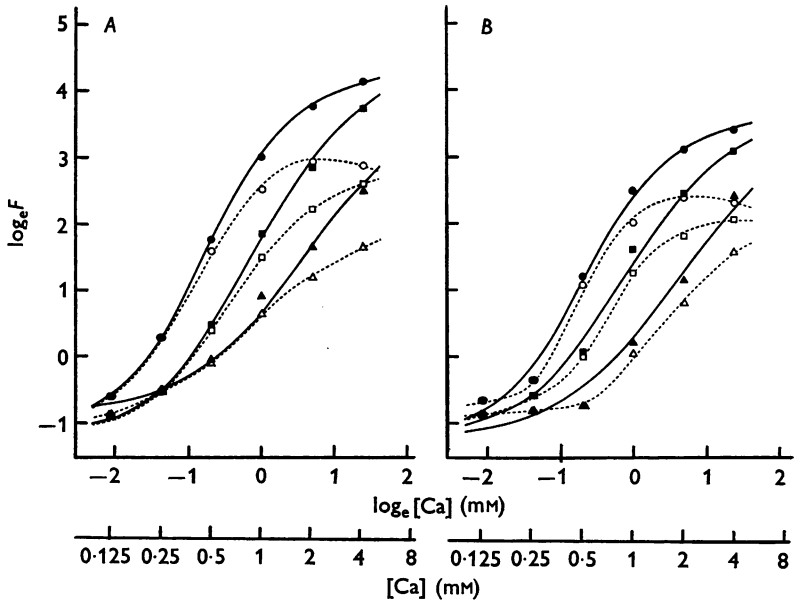

Fig. 8. Graphs of log F *vs.* log[Ca] at 1, 2, and 4 mM-Mg^{2+} (circles, squares, triangles respectively) in two hemi-diaphragms (part A and B) in 15 mM-K^+. Open symbols, mean log F's obtained by multiple sampling. S.E. of all points about 0·1 (range 0·08–0·13). Dashed lines fitted by eye. Filled symbols: data points adjusted for inhibition by Ca^{2+}. Continuous lines: theoretical curves with best-fitting parameters, for eqn. (4.3) (with $\theta = 2$, $\epsilon = 1$, 1·75, 3·25 for 1, 2 and 4 mM-Mg^{2+} respectively), except γ for both 4 Mg^{2+} curves set at 0·75.

i.e. that transmitter release is constant provided the function $(1+[Mg]/K)[Ca]^{-1}$ is constant, where K is the apparent dissociation constant of MgX. In the present experiments we were compelled to use raised [Mg] in order to follow the response of the quantal content of e.p.p.s to alteration of [Ca]. It was therefore necessary to verify whether in fact increase of [Mg] would simply act to cause parallel shifts of curves of log F *vs.* log[Ca], toward higher values of log[Ca].

The data shown in Fig. 8 are from two diaphragms in which m.e.p.p. frequencies were estimated by multiple sampling at a series of [Ca] concentrations, in 1, 2 and 4 mM-Mg^{2+} ([K^+] = 15 mM). These data show that raised [Mg] does indeed shift curves of log F *vs.* log [Ca] towards higher values of [Ca]. However, the data also show distinct flattening of the curves with increase of [Mg]. Thus, with the 'log' model (eqn. (4.2)), the best fitting θ's in the first diaphragm were 1·6, 1·3, and 1·05, in 1, 2 and 4 mM-Mg^{2+}, respectively, and in the second diaphragm θ's were 2·2, 1·95 and 1·6 respectively. Because of the lack of points at high values of [Ca] fitting to the 'linear' model was not possible but, from previous data, reduction of the maximum $\Delta \log F / \Delta \log [Ca]$ is associated with a reduction of θ in the 'linear' model. Correspondingly, graphs of [Ca] *vs.* [Mg] for constant F (cf. Jenkinson, 1957) showed a pronounced upward curvature, even with data adjusted for the inhibitory action of Ca^{2+}, which is inconsistent with the hypothesis of simple competition proposed by Jenkinson (1957).

To exclude the possibility that this result might be an artifact stemming from the inhibitory action of [Ca] (incompletely adjusted for) a series of experiments were done in which F was followed, with increasing [Ca], at five end-plates in 30 mM-K^+ and 5 mM-Mg^{2+}; the reduction in γ by raised [K^+] would allow fairly complete sigmoid curves to be obtained at relatively low concentrations of Ca^{2+}, where Ca inhibition is not appreciable. The results of this series did indeed show a consistent effect of raised [Mg] to flatten the curve of log F *vs.* log [Ca]. Fitting the data to the 'log' model, with θ 'floating', gave a mean θ of $1{\cdot}50 \pm 0{\cdot}19$, significantly ($P < 0{\cdot}05$) less than 2, the values previously obtained with 1 mM-Mg^{2+} (Table 1) and also significant ($P < 0{\cdot}01$) skewing of the curve of log F *vs.* log [Ca], even without adjustment for [Ca] inhibition. The deviations were consistent with eqn. (4.3), with a fit of the data optimum at $\epsilon \simeq 4$. From previous data $\epsilon = 1$ when [Mg] = 1. On the assumption that ϵ is linear with [Mg] (see Discussion) the solid lines drawn in Fig. 8*A* and *B* represent best fits of the adjusted data to eqn. (4.3), with ϵ set at 1, 1·75, and 3·25 for 1, 2 and 4 mM-Mg^{2+} respectively.

The increase in ϵ by Mg^{2+} only partially accounted for the shifts to the right of the curves of log F *vs.* log [Ca]. In the experiments with 15 mM-K^+, γ (found by fitting to eqn. (4.3) with appropriate ϵ) increased with [Mg], from 0·40 to 0·59 to 0·61 in one diaphragm and from 0·43 to 0·59 to 0·93 in the second diaphragm. The two values for 4 mM-Mg^{2+} were rather poorly defined, a value of 0·75 for both diaphragms in 4 mM-Mg^{2+} gave nearly as good fits and was used for the 'theoretical' curves in Fig. 8. Similarly, mean γ for the 30 mM-K^+, 5 mM-Mg^{2+} series was $0{\cdot}34 \pm 0{\cdot}02$, compared to $0{\cdot}13 \pm 0{\cdot}01$ in 30 mM-K^+, 1 mM-Mg^{2+}. From the 15 mM-K^+ data, when

different [Mg]'s were applied in the same diaphragm α and β were neither appreciably nor consistently altered.

Ca^{2+}-dependence of end-plate potentials

The Ca^{2+}-dependence of the quantal content of end-plate potentials was studied in two ways: (*a*) by multiple sampling of junctions in 1 mM-Mg^{2+}, and (*b*) by following individual junctions in 5 mM-Mg^{2+}. Multiple sampling was necessary for the experiment in 1 mM-Mg^{2+} because of the appearance of muscle twitching in low [Ca] solutions: in some cases muscle fibre thre-

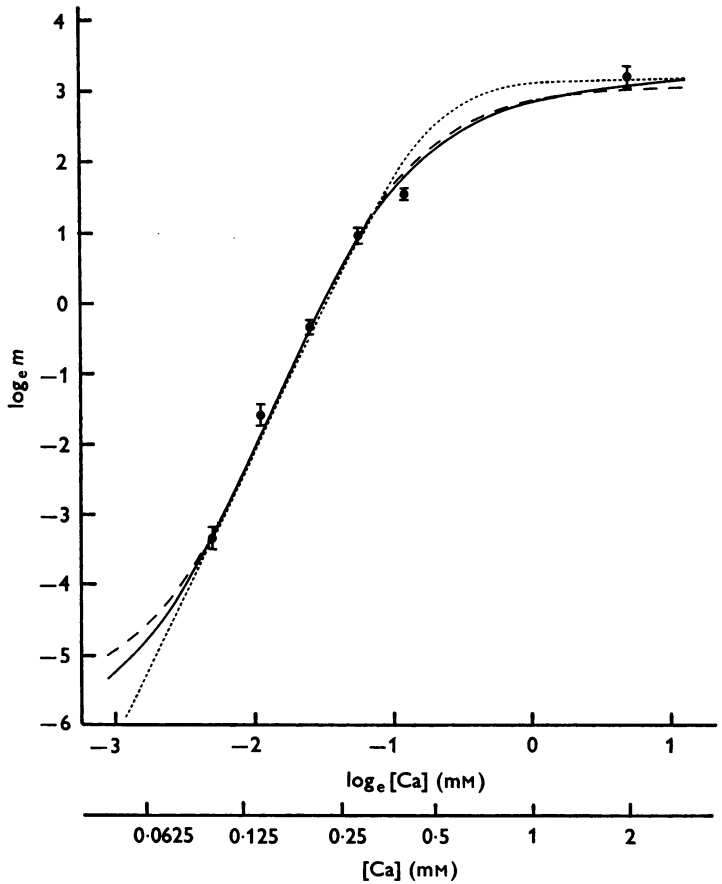

Fig. 9. Mean log quantal content of e.p.p.s ('*m*') *vs.* log [Ca] in a hemidiaphragm, nerve stimulated continuously at 10/sec. Some of e.p.p.s were recorded with added D-tubocurarine (range $0{\cdot}5 \times 10^{-7}$–2×10^{-7} g/ml.). Lines are theoretical curves with best-fitting parameters: continuous line: $\log m = \alpha + \beta\{1 + \gamma^2([Ca]^{-2} + [Ca]^{-1})\}^{-1}$; large dashes: $\log m = \alpha + \beta\{1 + \gamma^2 [Ca]^{-2}\}^{-1}$; small dashes: $m = \alpha + \beta\{1 + (\gamma[Ca]^{-1})^{\theta}\}^{-1}$. Note fit is closest to first equation, which provided best fit for m.e.p.p. frequencies in raised K^+.

shold was so low that even individual m.e.p.p.s generated action potentials. Unfortunately by this method it was impossible to obtain an unbiased estimate of mean log quantal content in very low [Ca]'s, because of uncertainty as to whether an apparent very low quantal content might represent failure of impulse conduction.

Fig. 9 shows means log quantal contents obtained in the presence of 1 mM-Mg^{2+}, with curves showing best fits to the 'linear' model and to the 'log' model (eqn. (4.3)). For comparison, the best fit to the 'log' model with $\theta = 2$ and $\epsilon = 0$ is also shown. Of these three curves, the best fit is provided by the modified 'log' model, with $\epsilon = 1$, and $\theta = 2$: these values were chosen solely on the basis of the results of the experiments in which release was evoked by raised [K^+]. The best fit for the 'linear' model was with $\theta = 4{\cdot}12$, i.e. the number of Ca^{2+} atoms that 'co-operate' for release of each quantum apparently may be more than 4. However, this fit was rather poor (mean square = 0·102, compared to 0·042 for the 'log' model) and not made significantly worse by choosing $\theta = 4$.

Examples of the relation between log quantal content (m) and log [Ca], obtained from end-plates in 5 mM-Mg^{2+}, are shown in Fig. 10. Although the total range of log [Ca] that could be tested was less than in the experiments using raised K^+ the sigmoid character of the curves was generally apparent and each series could be analysed separately in terms of the 'linear' and 'log' models. By the 'linear' model, mean θ for the total of eight end-plates followed was close to 4·0 ($3{\cdot}9 \pm 0{\cdot}2$), but fitting with θ held at four gave appreciably inferior best fits; the 'mean square' was more than doubled (from 0·013 to 0·027). As is apparent in Fig. 10, some of the end-plates demonstrated maximum slopes of $\Delta \log m / \Delta \log [Ca]$ appreciably more than 4, and others, less than 4. The best fit was provided by the 'log' model with θ free to vary (mean square = 0·008). However, this fit was not appreciably or significantly better than that provided by the 'log' model with $\theta = 2$, and $\epsilon = 4$, the same value of ϵ as fitted best the series of experiments using 30 mM-K^+ and 5 mM-Mg^{2+}. The best fitting θ, with θ 'floating' was $1{\cdot}45 \pm 0{\cdot}10$, much the same as with the 30 mM-K^+, 5 mM-Mg^{2+} data, indicating that raised Mg^{2+} causes the same deviation from eqn. (4.2) with e.p.p.s as with m.e.p.p. frequency evoked by raised K^+.

Another test of the goodness of fit of these models was provided by comparison of the extrapolated $\log m$ in 0-Ca^{2+}, i.e. $\log \alpha$ for the 'linear' model, and α for the 'log' model, with the observed $\log m$ in solution containing 0·1 mM-Ca^{2+} and 1 mM-EDTA (estimated free [Ca] $\simeq 10^{-3}$ mM, $\log_e$ [Ca] $\simeq -7$), which were successfully measured at four end-plates examined with 30·5/sec stimulation. In one of these quantal content was so low ($\log m \simeq -8{\cdot}1$) that only three 'successes' were evoked during 5 min stimulation. The best prediction of these quantal contents was obtained with the modified 'log' model with $\theta = 2$ and $\epsilon = 4$. It is of interest that comparing log m.e.p.p. frequency to $\log m$ showed an almost constant difference (6·6–6·9 $\log_e$ units) consistent with the notion that in this very low [Ca] solution there was no phasic acceleration of transmitter release by the nerve impulse, the 'quantal content' merely representing spontaneous m.e.p.p.s which occurred in the time period of

about 1 msec (see Methods) during which a m.e.p.p. was defined as an e.p.p. However, in other experiments it was observed that at most end-plates in this solution m.e.p.p. frequency increased with frequency of nerve stimulation, indicating that the nerve action potential was not blocked.

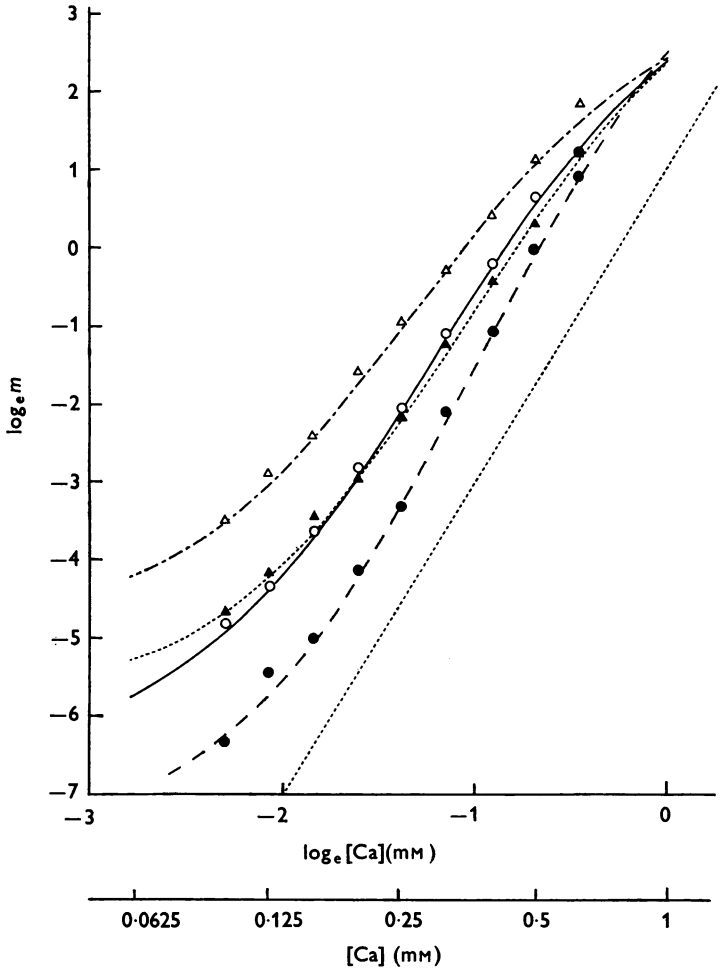

Fig. 10. Variation of log quantal content with log [Ca] at four end-plates stimulated at 30·5/sec. [Mg] = 5 mM. Dashes straight line drawn with slope of 4. Each curve represents best fit of data points to modified 'log' model, i.e. $\log m = \alpha + \beta\{1 + \gamma^2([\mathrm{Ca}]^{-2} + 4[\mathrm{Ca}]^{-1})\}^{-1}$.

Ca^{2+}-dependence of m.e.p.p. frequency increase evoked by focal polarization of nerve terminals

The determination of the Ca^{2+}-dependence of m.e.p.p. frequencies evoked by focal depolarization of nerve terminals (cf. Cooke & Quastel, 1972*a*) was made difficult by a tendency of the polarizing electrode grad-

ually to drift away from its best placement. The data shown in Fig. 11 are from one of two end-plates in which an estimate of local field *vs.* polarization, based on measurement of m.e.p.p. amplitude (Cooke & Quastel, 1972*a*) showed that the ratio of local field to current applied (which in this case was 7 mV per each 0·24 μA current step) could not have varied, during the series, by more than about 5 %. The graphs of Fig. 11*A* show much the same effect of low [Ca] as reported by Landau (1969) who used electrotonic

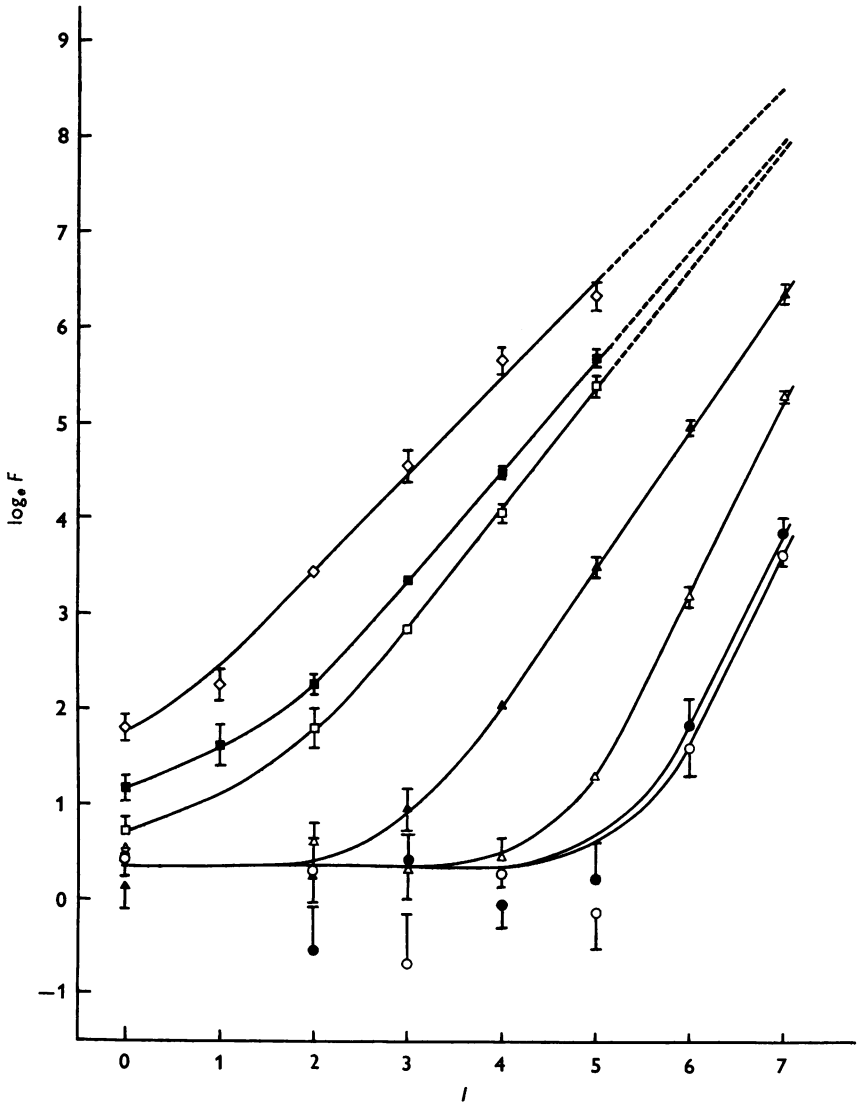

Fig. 11*A*. For legend see facing page.

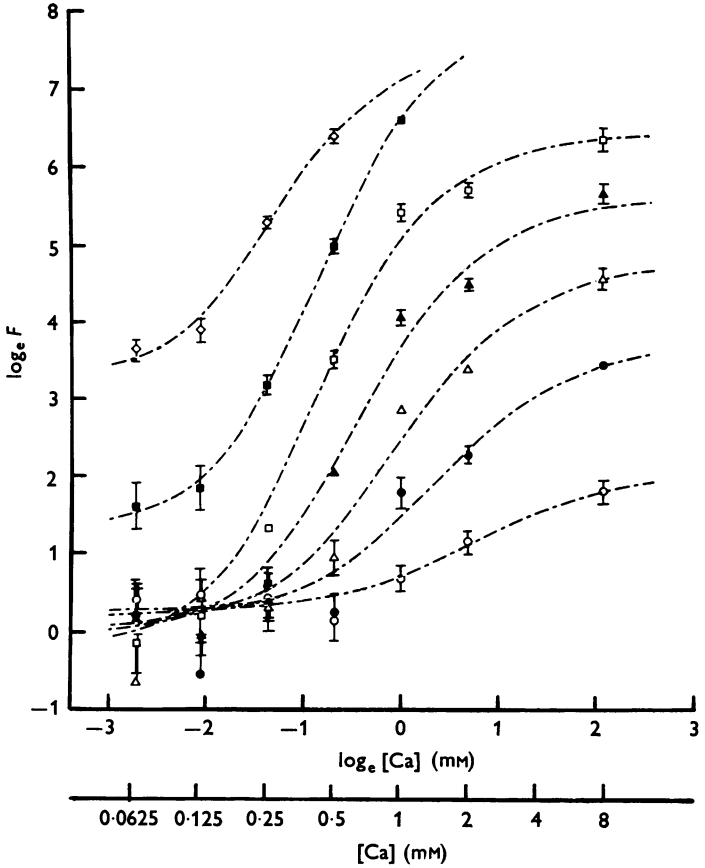

Fig. 11*B*.

Fig. 11 *A*. Relation between log F and focally applied current (arbitrary units, each equal to $-0{\cdot}24\ \mu$A) at an end-plate in 5 mM-K^+. Polarizations applied sequentially in 0·0625, 0·125, 0·25, 0·5, 1, 2, 8 mM-Ca^{2+} respectively (curves shift upward with increasing [Ca]). Each point is from one series only, except for points for $I = 4$, 5 in 2 mM-Ca^{2+} which are means from two determinations, one from before switching to low Ca^{2+}. Points without standard errors found by interpolation (m.e.p.p. size $\sim$ 0 due to extracellular field). These points were at progressively lower values of I because of progressive loss of muscle fibre membrane potential during the experiment. Note shift of curves to right and increase of maximum $\Delta \log F/\Delta I$, with reduction of [Ca]. Lines drawn by eye.

B, data from Fig. 11*A* plotted as log F *vs.* log [Ca], for, in ascending order, $I = 0, 2, 3, \ldots, 7$ arbitrary current units. Curves drawn are theoretical curves with parameters best fitting eqn. (4.3), with $\epsilon = 1$.

C, derived data from data of Fig. 11*A*. Graph of log γ *vs.* I (arbitrary units) found by fitting to eqn. (4.3), with $\epsilon = 1$. Line is best fitting linear regression line.

D, graph of α and β *vs.* I. β: triangles, α: circles. Both parameters found by least-squares fitting to eqn. (4.3), with $\epsilon = 1$.

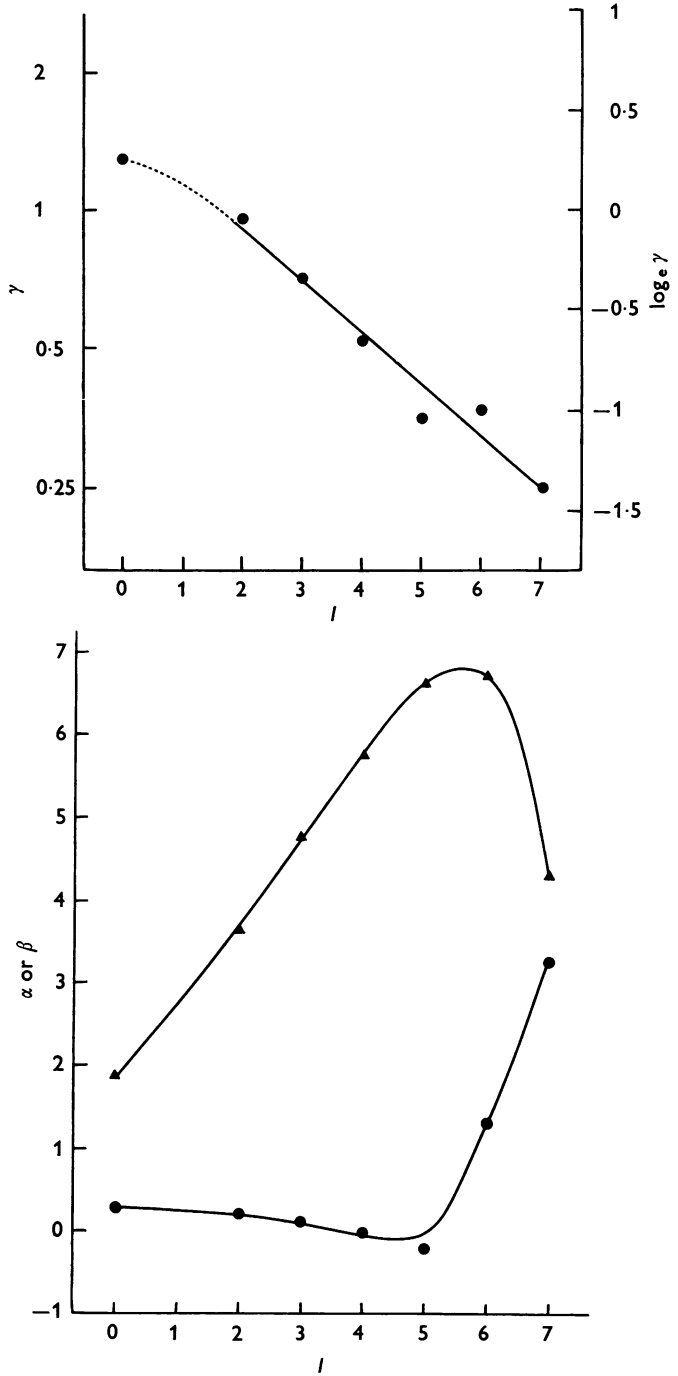

Fig. 11 *C*, *D*. For legend see previous page.

polarization: a shift to the right of curves of $\log F$ *vs.* I, with no reduction of maximum slope. Indeed there appears a consistent trend towards increased maximum slope of $\Delta \log F/\Delta I$ as [Ca] is reduced. The corresponding graph of $\log F$ *vs.* log [Ca] is shown in Fig. 11*B*.

As with other data from individual end-plates, these data were not in themselves sufficiently accurate to define a best-fitting model. However, they were well fitted by the modified 'log' model ($\theta = 2$, $\epsilon = 1$) which was previously found to apply to experiments where transmitter release was evoked by raised [K^+]. Derived parameters are plotted in Fig. 11*C* and *D*. As with increasing [K^+] (compare Fig. 7), γ falls with depolarization, while β at first rises with depolarization and subsequently falls. A major effect, only hinted at in the data from the experiments with raised [K^+] (see Fig. 7) is a striking rise in α with the greater depolarizations. In the other successful experiment using focal polarization, at [K^+] = 20 mM, very similar results were obtained.

In both experiments $\log \gamma$ appeared to fall linearly with depolarizing current, over the whole range for the end-plate in 20 mM-K^+, and with current greater than two units (corresponding to -14 mV extracellular field) in the other. The slopes of these lines were $-0{\cdot}078$ and $-0{\cdot}259$ per current unit respectively. The corresponding slopes of $\log F$ *vs.* current at the two end-plates were 0·435 and 1·2, in 2 mM-Ca^{2+}. Thus the two values of $\Delta \log \gamma/\Delta \log F$ were similar: $-0{\cdot}179$ and $-0{\cdot}216$ respectively. From previous data (Cooke & Quastel 1972*a*, *c*) the true slope $\Delta \log F/\Delta V$ in 2 mM-Ca^{2+} (V is presynaptic membrane potential), was calculated to be between 0·16/mV and 0·24/mV, and was about 25% higher in 20 mM-K^+. Using these values, $\Delta \log \gamma/\Delta V$ in these two experiments was between $-0{\cdot}036$ and $-0{\cdot}054$/mV and between $-0{\cdot}035$ and $-0{\cdot}052$ respectively. These estimates can be compared with the slope of $-0{\cdot}053$/mV found from experiments using raised K^+ to evoke transmitter release (Fig. 7*B*).

Non-independence of derived parameters: correlation of β and γ with α

In the experiments in which the response of end-plate potential amplitude to [Ca] was followed at individual end-plates it was noted that with stimulation at 30/sec m.e.p.p. frequency varied greatly from end-plate to end-plate. Indeed, at the occasional junction m.e.p.p. frequency was as high as 100/sec, and this frequency was not rapidly suppressed in low Ca^{2+}-EDTA solution. At such junctions it was not possible to estimate e.p.p. quantal content with any accuracy, and the results were not suitable for analysis. However, it appeared that the response of quantal content to [Ca] was rather small. At the junctions which were accurately followed a relatively high m.e.p.p. frequency seemed to be associated not only with a high 'basal' quantum content (in the EDTA solution), but also with a relatively small range of alteration of log quantal content by Ca^{2+} (Fig. 10). That is, with α and β calculated by the 'log' model, high α was associated with low β. Examination of the derived data from the experiments using raised [K^+] showed, for each series, a negative correlation of β *vs.* α that was significant at the 5% level at seven and at the 1% level at four of the total of eight series. Fig. 12*A* shows a plot of the relation between α and β from the experiments with 15 mM-K^+ and 20 mM-K^+, as well as the e.p.p. data. By extrapolation, it would appear possible that in all cases β would become 0 if α were to increase to about 7 (i.e. Ca independent $F \simeq 1000$/sec). This finding suggests that the decline

in β that occurs with large depolarizations (Figs. 7*B*, 11*D*) may be linked to concurrent rise in α. Moreover, it recalls the uncoupling phenomenon reported previously (Cooke & Quastel, 1972*b*), i.e. that when m.e.p.p. frequency at a junction is high after a large focally applied depolarization, the responsiveness of m.e.p.p. frequency to depolarization is depressed.

In no one set of experiments was there any significant correlation of γ or log γ with α or β. However, it was observed that the slopes of the regression lines appeared to permute regularly with $[K^+]$ or mean log γ; Fig. 12*B* shows how the slope of the regression line of log γ *vs.* α correlates (r = 0·97) with mean log γ.

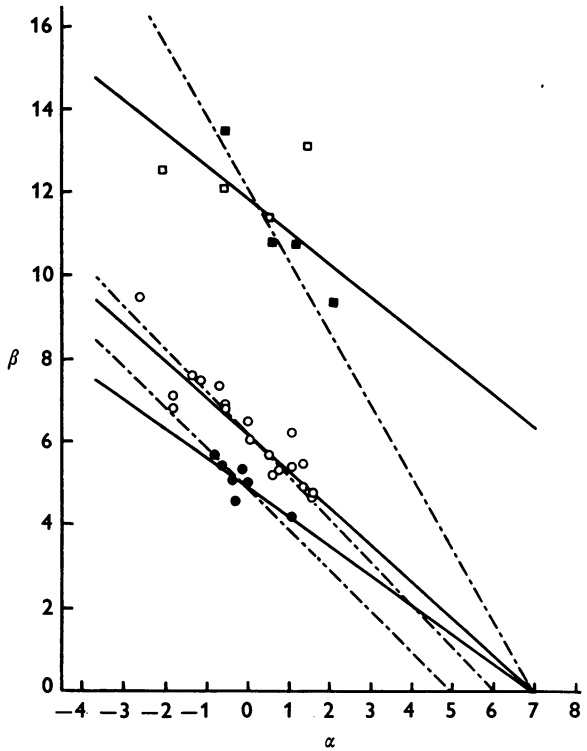

Fig. 12A. For legend see facing page.

Focal polarization of nerve terminals – brief pulses

From Fig. 11*A* it is evident that when nerve terminals are depolarized by focally applied current (I) the maximum slope of $\Delta \log F/\Delta I$ is increased rather than decreased by low Ca^{2+}. However, these experiments were performed using polarizing pulses up to several seconds in duration. From previous work (Cooke & Quastel, 1972*b*) such pulses evoke a cumulative and persistent response of m.e.p.p. frequency requiring very little Ca^{2+}, as well as a phasic response. If this slow response were to correspond to increase of α, and raised α were associated with a reduction of β (Fig. 12*A*),

then, with *brief* depolarizing pulses one would expect a continuing rise of β with depolarization, and correspondingly an increase in maximum $\Delta \log F/\Delta I$ with increasing [Ca]. This experiment proved difficult: because of the necessity of using very large depolarizing pulses muscle movement

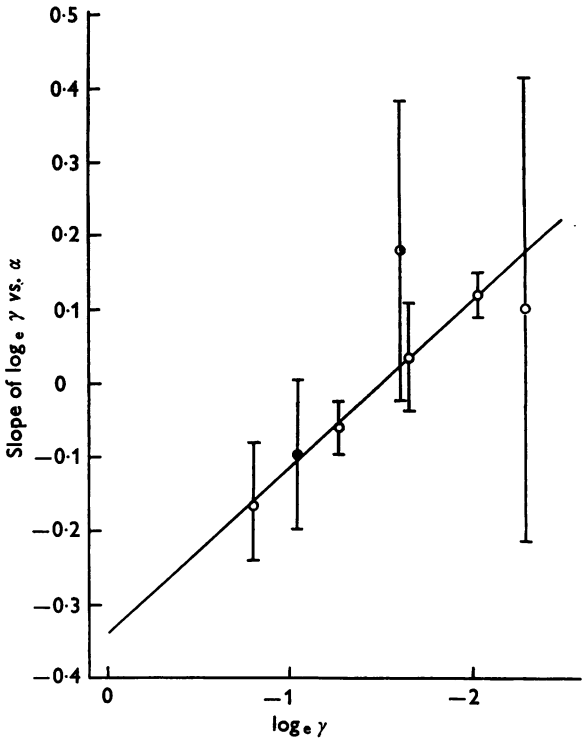

Fig. 12*B*.

Fig. 12 *A*, correlations between β and α (eqn. (4.3)) from experiments in 15 mM-K^+ (●), 20 mM-K^+ (○) and end-plate potentials (6·8 added to true α to make it equivalent to basal log m.e.p.p. frequency, ■: 30·5/sec, □: 5/sec). In each case continuous line is regression line for β *vs.* α and interrupted line is regression line for α *vs.* β. Note data compatible with intersection of lines at $\beta = 0$, $\alpha \simeq 7$. These variations of α and β are more than tenfold that which can be attributed to inaccuracy of individual estimations of m.e.p.p. frequency; this correlation is therefore not an artifact secondary to least-squares fitting procedures.

B, graph of the slope of regression lines of log γ *vs.* α, plotted *vs.* log γ. Although individual slopes are not significant, there is a significant regression of these values with log γ ($r = 0{\cdot}97$). (○): from series of experiments in 15, 20, 25, 30, 50 mM-K^+, from left to right. (●): 20 mM-K^+, 50 m-osmole hypertonic. (◑): 20 mM-K^+, 50 m-osmole hypotonic.

Plot *vs.* log γ permits inclusion of data with varied osmotic pressure, otherwise plot *vs.* log [K^+] or nominal membrane potential would be virtually identical.

TABLE 3*A*. The effect of increasing [Ca] from 0·25 to 0·5 mM in the presence of 3 mM-Mg^{2+}, on transmitter release evoked by steady depolarization and superimposed 25 msec pulses. Data averaged from those presented in Fig. 13*C*.

			log *F*			
	I (μA)	V_0 (mV)*	0·25 mM-Ca (Control)	0·5 mM-Ca (5–10 sec)	0·25 mM-Ca (5–40 sec)	$\frac{\Delta \log F\dagger}{\Delta \log [Ca]}$
Basal	−27·2	−72	2·73 ± 0·03	4·74 ± 0·05	2·85 ± 0·05	2·90 ± 0·06
Smaller pulse	−31·2	−83	3·39 ± 0·11	5·72 ± 0·12	3·45 ± 0·15	3·36 ± 0·23
Larger pulse	−35·7	−95	3·92 ± 0·08	6·52 ± 0·08	3·86 ± 0·12	3·75 ± 0·16

B. Same data as Table 3*A*, expressed in the form of the changes of $\Delta \log F/\Delta V_0$ caused by the added pulses

	Added pulse		$\Delta \log F/\Delta V_0$			
	ΔI (μA)	ΔV_0 (mV)	0·25 mM-Ca	0·5 mM-Ca	0·25 mM-Ca	$\frac{\Delta \log F, 0{\cdot}5\ Ca\dagger}{\Delta \log F, 0{\cdot}25\ Ca}$
Smaller pulse	−4	−11	0·060 ± 0·010	0·090 ± 0·011	0·055 ± 0·012	1·48
Larger pulse	−8·5	−23	0·052 ± 0·004	0·078 ± 0·004	0·044 ± 0·006	1·49

* V_0 = local extracellular field calculated on basis of transmitter equilibrium potential of −10 mV, and m.e.p.p. amplitudes.

† Calculated from data for 0·5 mM-Ca^{2+} at 5–10 sec after changing solution and for 0·25 mM-Ca^{2+} averaged over several minutes *before* the change.

could be avoided only by pre-treatment with glycerol (Howell, 1969), which resulted in a very low muscle membrane potentials. Results from two successful experiments are shown in Fig. 13, and Table 3. With increase of [Ca] from 0·25 to 0·5 mM there was in both experiments increase of $\Delta \log F/\Delta I$, by almost 50% in the second experiment (Table 3*B*). Conversely, $\Delta \log F/\Delta \log [Ca]$ was graded with depolarization (Table 3*A*). It should be noted that the m.e.p.p. frequency elicited by the basal depolarization, in the second experiment, was 15/sec ($\log F = 2{\cdot}73$), well above the level at which curves of $\log F$ *vs.* current show upward curvature (compare Fig. 11*A*). Thus, the increase of $\Delta \log F/\Delta \log [Ca]$ with depolarization must be attributed to increase of β rather than reduction of γ, although the m.e.p.p. frequencies achieved indicate that the higher depolarization used was in the range associated with reduction of β when prolonged depolarization pulses were used for testing. In the second experiment, $\Delta \log F/\Delta I$ was not the same for the two pulses, suggesting that at such high levels of depolarization (probably ~ 40 to 60 mV depolarization) the slope of $\log F$ *vs.* membrane potential progressively declines. The change of [Ca] increased both values of $\Delta \log F/\Delta I$ by the same factor (Table 3*B*).

DISCUSSION

The relation between transmitter release and extracellular Ca^{2+} concentration is very obviously a function of presynaptic membrane potential. With increasing depolarization, either by raised $[K^+]$ or extrinsic current applied focally to the end-plate (compare Figs. 5 and 11*B*) the curve of log m.e.p.p. frequency *vs.* log [Ca] retains its sigmoid shape, but is shifted upward and to the left. For at least small depolarizations, there is also a marked increase in the range through which m.e.p.p. frequency (F) alters with [Ca]. Interpreted in terms of the 'linear' model (see Theory), this increase of the Ca-dependent component of F was associated with an apparent increase in θ, the number of Ca atoms involved in the complex(es) that activate release in all-or-nothing fashion, over a range from unity to at least four. This result contradicts the hypothesis that any fixed number of Ca^{2+} atoms always 'co-operate' in release of a quantum of transmitter. It may be noted that the equation for the linear model (eqn. (4.1)) becomes, with simplification, the same as one of the equations of Dodge & Rahamimoff (1967) or the equation of Hubbard *et al.* (1968*b*).

In contrast, all data were well fitted by the equation of the 'log' model, with constant θ, consistent with the hypothesis that a Ca complex activates transmitter release in a continuously graded, rather than all-or-nothing fashion. It is in general true that any set of data points that fits eqn. (4.2) (or eqn. (4.3), with small ϵ) can also be fitted rather closely, and within

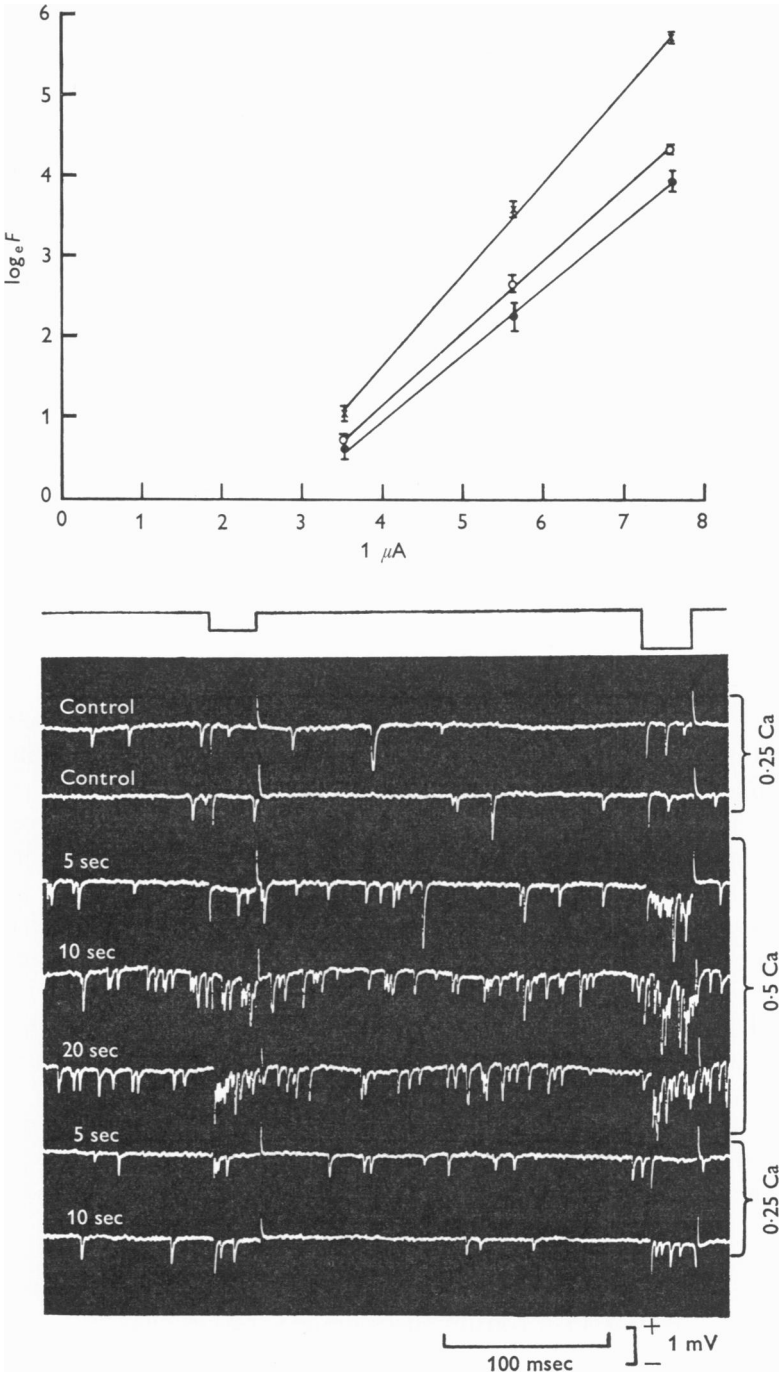

Fig. 13*A*, *B*. For legend see facing page.

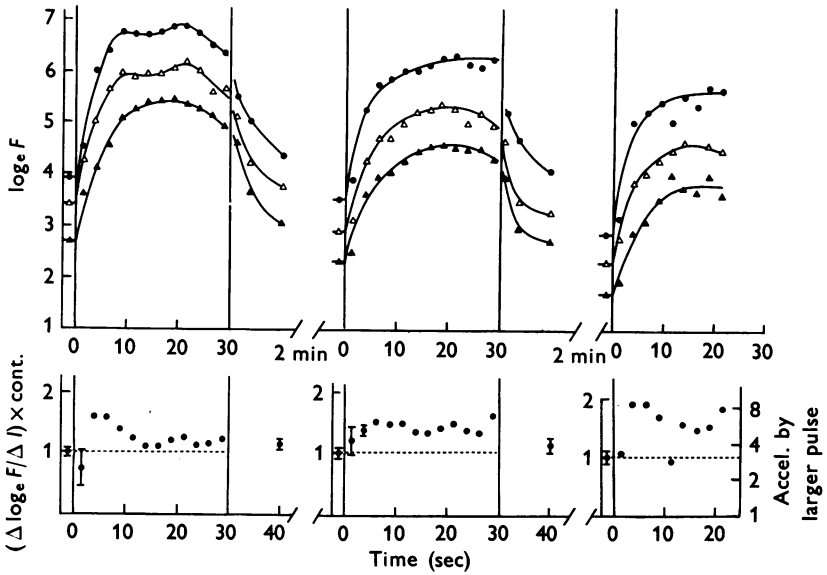

Fig. 13*C*.

Fig. 13. *A*, effect of raised [Ca] on relation between log *F* and focal depolarizing current. Current of $-3{\cdot}5\ \mu$A was applied continuously and added pulses of $-2\ \mu$A and $-4\ \mu$A of 25 msec duration were alternated. Points in 0·25 Ca^{2+}, 3 mM-Mg^{2+} (open circles) represent averages over period of several minutes. Points for 0·5 mM-Ca^{2+}, 3 mM-Mg^{2+} (crosses) are averages for period 20–60 sec after changing solution. Filled circles – after 1 min return to 0·25 mM-Ca^{2+}, 3 mM-Mg^{2+}, averaged over one minute period. Bars indicate ± S.E. of mean.

B, samples of record from experiment similar to that of *A*. Top line indicates time sequence of pulses superimposed on 'basal' depolarization. Note transients on records corresponding to beginning and end of each pulse. All m.e.p.p.s were inverted as a result of local extracellular fields. With doubling of [Ca] (0·25 mM to 0·5 mM, [Mg] was 3 mM) m.e.p.p. frequencies increased, especially during pulses.

C, *top portion*. Same experiment as Fig. 13*B*. Graph of log *F* *vs.* time for basal frequency (▲) and for small and large pulses (△ and ● respectively), for three iterations of 30 sec switch from 0·25 to 0·5 mM-Ca^{2+}, in 3 mM-Mg^{2+}. Each point represents average from five pulses, except for control (0·25 mM-Ca^{2+}) values, which each represent averages over period of 1 min. During course of experiment there was small drift of polarizing electrode away from end-plate resulting in progressively lower values of log *F* for each current.

Lower portion: Ratio of $\Delta \log F/\Delta I$ in 0·5 mM-Ca^{2+} to $\Delta \log F/\Delta I$ in 0·25 mM-Ca^{2+}, for the larger pulse. Standard error bars for a few points in 0·5 mM-Ca^{2+} are drawn, to indicate approximate error range of estimate of this ratio. Data derived from upper portion of this Figure.

experimental error, to eqn. (4.1). The reverse does not hold, i.e. unless relative values of α, β and θ are properly chosen sets of points fitting the 'linear' model (eqn. (4.1)) tend to fit eqn. (4.2) extremely badly, and θ has no particular tendency to have the value of 2, or indeed, any integral value. The failure of the 'linear' model to predict the observed good fit to the 'log' model is a strong reason for preferring the latter and rejecting the former.

The 'linear' model. Eqn. (4.1), of course, represents a simplification of eqn. (3.1), i.e. a quotient of polynomials, each of which, for this model, extends to terms at least as high as $[Ca]^4$ and probably to $[Ca]^5$. There is no way in which the data can contradict the hypothesis that this expression does in fact represent reality, the various coefficients just happening to permute with depolarization in such a way that a fit to eqn. (4.3) (i.e. to the 'log' model) is always maintained. It should not be thought that this could arise simply as a result of depolarization acting to permit Ca^{2+} entry into the nerve terminal, high order Ca complexes being formed simply as a result of more Ca^{2+} being present. On the contrary, whatever the function linking intracellular Ca concentration to transmitter release, a simple increase of Ca^{2+} permeability could do no more than a proportional increase of extracellular Ca concentration. In short, only γ could be altered by this mechanism, not β or θ. Rise in θ and β demands the postulate that with increasing depolarization higher order Ca complexes or Ca^{2+} atoms from such complexes become active in stimulating quantal release, and moreover, either that depolarization alters Ca^{2+} receptor(s) in such a way as to promote formation of the higher order Ca complexes or that the complex of each order involves a different receptor. It may be pointed out that once it is supposed that depolarization can alter affinity of Ca^{2+} receptor(s) for Ca^{2+} there is no need to postulate Ca^{2+} entry into the nerve terminal to account for change of γ or acceleration of transmitter release (cf. Dodge & Rahamimoff, 1967; Hubbard *et al.* 1968*b*). To account for the phenomenon of increase of α with depolarization, and, at high depolarizations, the concomitant reduction of β with α (and indeed variation in θ paralleling that of β) requires the further assumption of an effect of depolarization similar to that put forward to supplement the 'log' model (see below).

The 'log' model. The manner in which the parameters of the log model equation were found to vary with presynaptic depolarization does not confirm to any single prediction of the Ca-hypothesis (see Theory) but can be easily accommodated to it. The alteration of γ with depolarization strongly suggests that a Ca complex that acts as a graded activator of release is formed within the nerve terminal, where access of Ca ions is governed by presynaptic membrane potential. Alteration of β with membrane potential may be explained in at least two ways: (*a*) the amount of Ca 'receptor' in the nerve terminal increases with depolarization, and/or (*b*) Ca entry is governed by the amount of a Ca complex in or on the nerve terminal membrane. Choosing the second alternative as the more plausible, there are only two alternatives that fit the data: (*a*) the external Ca complex governing Ca entry requires two Ca atoms and the internal Ca complex only one, or (*b*) the converse – one Ca atom attaches to the external receptor and two to the internal. The only evidence on which to decide

between these possibilities is that pertaining to ϵ. When kinetic models are set up in which Mg^{2+} competes with Ca^{2+} at all binding sites it is found that only the first alternative is compatible with a value of ϵ which does not rise markedly with depolarization (i.e. with reduced γ), and rises fairly linearly with [Mg]. Similarly, models in which Ca^{2+} enters the nerve terminal in proportion to extracellular Ca^{2+}, but Ca permeability is inhibited by a Ca^{2+} complex, can be constructed in such a way as to predict the empirical formula (4.3) and rise of β as well as reduction of γ with depolarization, but predict behaviour of ϵ difficult to reconcile with the observed data.

The model that remains, i.e. Ca entry proportional to the amount of a Ca_2Y on the membrane and governed by presynaptic membrane potential, and a CaX inside the terminal that activates release in graded fashion, does not account for the observed increase of α with depolarization. Since increase of α appears to be associated with a reduction in β, one explanation for the phenomenon is that the internal Ca receptor (X) may be transformed, as a result of depolarization, into a form (X′) which needs no Ca^{2+} attached to it in order to activate release. This would account for the phenomenon of 'inactivation' or 'uncoupling', described in a previous paper (Cooke & Quastel, 1972*b*). If the extent of $X \rightarrow X'$ transformation were to vary from one nerve terminal to another the observed negative correlation between α and β would follow.

This model also fails to account fully for the extent to which β increases with depolarization.

On the assumption that internal Ca ($[Ca]_i$) is proportional to an external $[Ca_2Y]$ and a function of membrane potential, i.e.

$$[Ca]_i = f(V)[Ca_2Y],$$
$$\log F = a_0 + a_1X_t\{1 + K_3f(V)^{-1}[Ca_2Y]^{-1}\}^{-1}$$
$$= a_0 + a_1X_t\{1 + K_3f(V)^{-1}Y_t^{-1}(1 + K_2[Ca]^{-1} + K_1K_2[Ca]^{-2})\}^{-1}$$

equating coefficients with those of eqn. (4.3), one obtains

$$a = a_0, \quad \beta = a_1X_t\{1 + K_3f(V)^{-1}Y_t^{-1}\}^{-1},$$
$$\gamma^2 = K_1K_2K_3\{K_3 + f(V)Y_t\}^{-1}, \quad \epsilon = K_1^{-1},$$

where K_1, K_2, K_3 are dissociation constants (Mg competition is accommodated by changes in these parameters) a_0, a_1, X_t, and Y_t are constants.

Thus, $\beta = a_1X_t(1 - \gamma^2K_1^{-1}K_2^{-1})$.

That is, the model predicts a linear relation between β and γ^2, extrapolating to $\beta = a_1X_t$ when $\gamma^2 = 0$ and to $\gamma^2 = K_1K_2$ when $\beta = 0$. Fig. 14*A* and *B* show graphs of β *vs.* γ^2, for the series with various $[K^+]$ and the two end-plates that were polarized focally. It is evident that the relation between β and γ^2 is not linear. In view of the possibility that high α may entail low β (Fig. 12*A*) $\alpha + \beta$ is also plotted *vs.* γ^2: the result only empha-

sizes that β (or $\alpha+\beta$) rises with depolarization (i.e. with reduced γ^2) to a greater extent than predicted. In short, the data suggest that increase of Ca entry with depolarization cannot account entirely for the extent by which transmitter release is increased by nerve terminal depolarization. An increase of the available internal Ca receptor is suggested. This hypothesis, that the high rate of transmitter release that can be evoked by depolarization requires increase of intracellular X_t as well as intracellular Ca^{2+}, is in keeping with the failure of Miledi & Slater (1966) to elicit transmitter release by injection of Ca^{2+} into the giant nerve terminal in the squid stellate ganglion.

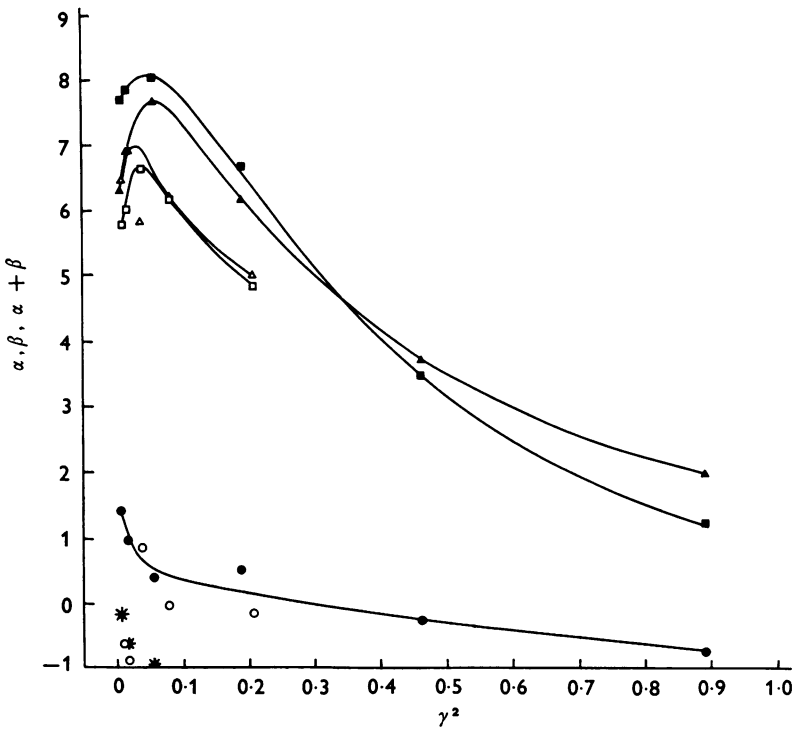

Fig. 14*A*. For legend see facing page.

Correlation of parameters. The observation that α, β and γ are not independent (Fig. 12*A*, *B*) suggests that modification of these parameters by depolarization may be closely linked. If we attribute the rise in α to formation of X' from X, the large variation of α in K^+-depolarized or tetanized nerve terminals could reflect differences in rate of formation or of disposal of X'. At low levels of depolarization $\log\gamma^{-2}$ is positively correlated with α (Fig. 12*B*). This suggests that terminals with high α may simply be terminals either more depolarized than others, or more responsive to depolarization. With high depolarization, on the other hand, there appears a negative correlation of $\log\gamma^{-2}$ with α, suggesting that high α may itself entail a tendency for

Ca permeability to become reduced. If we are correct in identifying raised α with the increase in m.e.p.p. frequency that persists after a large presynaptic depolarization (Cooke & Quastel, 1972*c*) then the concurrent 'inactivation' or 'uncoupling' of responsiveness of m.e.p.p. frequency to depolarization may reflect not only reduced β, but also, to a relatively small extent, reduction of the responsiveness of Ca entry to depolarization.

It may be recalled that the rise in m.e.p.p. frequency that follows a large depolarization depends upon the presence of a small amount of Ca^{2+} (Cooke & Quastel, 1972*b*). In the present experiments α was always close to the m.e.p.p. frequency in '0' Ca^{2+} (0·1 mM-Ca^{2+}, 1 mM-MgEDTA) in the experiments using raised K^+ or nerve impulses

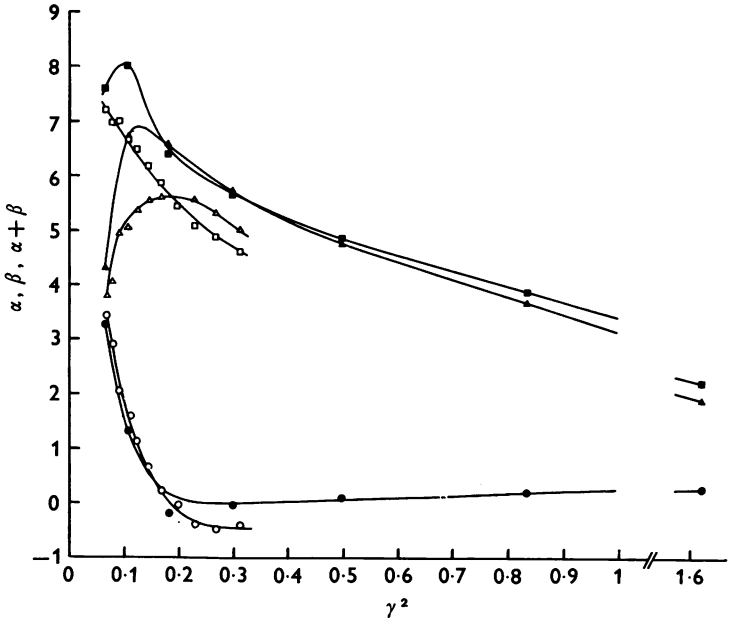

Fig. 14*B*.

Fig. 14 *A*. Same data as Fig. 7*A* and *B*, with α (circles), β (triangles) and $\alpha+\beta$ (squares) plotted *vs.* γ^2.

Open symbols, means from 'followed' end-plates. Filled symbols, data from multiple sampling experiments.

B, similar to *A* with data from end-plate polarized in 20 mM-K^+ (open symbols) and end-plate polarized in 5 mM-K^+ (filled symbols).

Note similarity of curves (drawn by eye) and non-fit to linearity between β (or $\alpha+\beta$) and γ^2, as predicted by the model (see text) in which β increases because of increase of Ca entry by depolarization.

(maintained throughout at a steady rate) to stimulate release. However, in one of the experiments using focal polarization m.e.p.p. frequencies in '0'-Ca^{2+} were much lower than the α's found by curve fitting. This result is in keeping with the notion that the rise of α with depolarization requires a small amount of Ca^{2+} for its development, but can be maintained for a considerable time in the virtual absence of extracellular Ca^{2+}.

Relation between Ca entry and depolarization. On the assumption that the effect of raised K^+ on γ is related solely to nerve terminal depolarization, the slope of $\log\gamma$ *vs.* V_m ('log' model) was $-0{\cdot}053$/mV, and the values of $\log\gamma$ *vs.* V_m were the same at focally polarized end-plates provided $\Delta\log F/\Delta V_m$ normally (in 5 mM-K^+ and 2 mM-Ca^{2+}) is 0·24/mV, a maximum estimate from previous data (Cooke & Quastel, 1972*a*). However, the specific action of K^+ to potentiate the response to depolarization (Cooke & Quastel, 1972*c*) is compatible with an action of K^+ to increase the sensitivity of Ca entry to depolarization, and such an action is suggested by the finding of γ as low in high K^+ (30 and 50 mM) as with end-plate potentials. If this is indeed the case the slope of $\log\gamma$ *vs.* V_m calculated from raised K^+ data will be too high. The true slope might be as low as $-0{\cdot}04$/mV, corresponding to true $\Delta\log F/\Delta V_m \sim 0{\cdot}18$/mV. If Ca entry is governed by the amount of a Ca_2Y on the membrane, rather than free Ca or a single order Ca complex, the ratio of $[Ca]_{in}$ to $[Ca_2Y]$ is very nearly proportional to γ^{-2}. On this basis a slope of $\log\gamma$ *vs.* V_m of $-0{\cdot}04$/mV indicates an e-fold increase of Ca entry per 12·5 mV depolarization, perhaps corresponding to the amount of a doubly charged molecule on one face of the membrane. If true $\Delta\log F/\Delta V_m$ (in standard 5 mM-K^+ and 2 mM-Ca^{2+}) is 0·24/mV, Ca entry increases e-fold per 9·4 mV depolarization.

Magnesium. In terms of the model put forward above, in which an extracellular Ca_2Y governs Ca entry and an intracellular CaX mediates transmitter release, the actions of raised [Mg] are compatible with competition of Mg^{2+} with Ca^{2+} at both the intracellular site (where it increases γ) and the extracellular site (where its main effect is to increase ϵ).

The data of Jenkinson (1957) and of Dodge & Rahamimoff (1967) also show deviations from the simple competitive model (downward curving plots of [Ca] *vs.* [Mg] for equal '*m*') suggestive of a further effect of Mg^{2+} on release, perhaps to prolong 'facilitation' (see Cooke & Quastel, 1972*b*), which would obscure the double action seen in the present experiments. The present hypothesis is supported by the finding of Douglas & Poisner (1964) that, in the neurohypophysis, the inhibition of Ca^{2+} entry by Mg^{2+} was insufficient to account for inhibition of vasopressin secretion.

This work was supported by grants from the Muscular Dystrophy Association of Canada and the Medical Research Council.

REFERENCES

COOKE, J. D. & QUASTEL, D. M. J. (1973*a*). Transmitter release by mammalian motor nerve terminals in response to focal polarization. *J. Physiol.* **228**, 377–405.

COOKE, J. D. & QUASTEL, D. M. J. (1973*b*). Cumulative and persistent effects of nerve terminal depolarization on transmitter release. *J. Physiol.* **228**, 407–434.

COOKE, J. D. & QUASTEL, D. M. J. (1973*c*). The specific effect of potassium on transmitter release by motor nerve terminals and its inhibition by calcium. *J. Physiol.* **228**, 435–458.

DEL CASTILLO, J. & ENGBAEK, L. (1954). The nature of the neuromuscular block produced by magnesium. *J. Physiol.* **124**, 370–384.

DEL CASTILLO, J. & KATZ, B. (1954). The effect of magnesium on the activity of motor nerve endings. *J. Physiol.* **124**, 553–559.

DEL CASTILLO, J. & STARK, L. (1952). The effect of calcium ions on the motor end-plate potentials. *J. Physiol.* **116**, 507–515.

DODGE, F. A. & RAHAMIMOFF, R. (1967). Cooperative action of calcium ions in transmitter release at the neuromuscular junction. *J. Physiol.* **193**, 419–433.

DOUGLAS, W. W. & POISNER, A. M. (1964). Calcium movement in the neurohypophysis of the rat and its relation to the release of vasopressin. *J. Physiol.* **172**, 19–30.

ELMQVIST, D. & FELDMAN, D. S. (1965). Calcium dependence of spontaneous acetylcholine release at mammalian motor nerve terminals. *J. Physiol.* **181**, 487–497.

FATT, P. & KATZ, B. (1952). Spontaneous subthreshold activity at motor nerve endings. *J. Physiol.* **117**, 109–128.

FENG, T. P. (1936). Studies on the neuromuscular junction. II. The universal antagonism between calcium and curarising agencies. *Chin. J. Physiol.* **10**, 513–528.

GAGE, P. W. & QUASTEL, D. M. J. (1966). Competition between sodium and calcium ions in transmitter release at a mammalian neuromuscular junction. *J. Physiol.* **185**, 95–123.

HOWELL, J. N. (1969). A lesion of the transverse tubules of skeletal muscle. *J. Physiol.* **201**, 515–534.

HUBBARD, J. I. (1961). The effect of calcium and magnesium on the spontaneous release of transmitter from mammalian motor nerve endings. *J. Physiol.* **159**, 507–517.

HUBBARD, J. I., JONES, S. F. & LANDAU, E. M. (1968*a*). On the mechanism by which calcium and magnesium affect the spontaneous release of transmitter from mammalian motor nerve terminals. *J. Physiol.* **194**, 355–380.

HUBBARD, J. I., JONES, S. F. & LANDAU, E. M. (1968*b*). On the mechanism by which calcium and magnesium affect the release of transmitter by nerve impulses. *J. Physiol.* **196**, 75–86.

HUBBARD, J. I., LLINÁS, R. & QUASTEL, D. M. J. (1969). In *Electrophysiological Analysis of Synaptic Transmission*, p. 132. London: Edward Arnold.

JENKINSON, D. H. (1957). The nature of the antagonism between calcium and magnesium ions at the neuromuscular junction. *J. Physiol.* **138**, 438–444.

KATZ, B. & MILEDI, R. (1965). The effect of calcium on acetylcholine release from motor nerve endings. *Proc. R. Soc.* B **161**, 496–503.

KATZ, B. & MILEDI, R. (1967). A study of synaptic transmission in the absence of nerve impulses. *J. Physiol.* **192**, 407–436.

KATZ, B. & MILEDI, R. (1969). Spontaneous and evoked activity of motor nerve endings in calcium Ringer. *J. Physiol.* **203**, 689–706.

KATZ, B. & MILEDI, R. (1970). Further study of the role of calcium in synaptic transmission. *J. Physiol.* **207**, 789–801.

LANDAU, E. M. (1969). The interaction of presynaptic polarization with calcium and magnesium in modifying spontaneous transmitter release from mammalian motor nerve terminals. *J. Physiol.* **203**, 281–299.

LILEY, A. W. (1956). The effects of presynaptic polarization on the spontaneous activity at the mammalian neuromuscular junction. *J. Physiol.* **134**, 427–443.

MILEDI, R. & SLATER, C. R. (1966). The action of calcium on neuronal synapses in the squid. *J. Physiol.* **184**, 473–498.

QUASTEL, D. M. J., HACKETT, J. T. & COOKE, J. D. (1971). Calcium: Is it required for transmitter secretion? *Science, N.Y.* **172**, 1034–1036.

QUASTEL, D. M. J., HACKETT, J. T. & OKAMOTO, K. (1972). Presynaptic action of central depressant drugs: Inhibition of depolarization-secretion coupling. *Can. J. Physiol. Pharmac.* **50**, 279–284.

RUBIN, R. P. (1970). The role of calcium in the release of neurotransmitter substances and hormones. *Pharmac. Rev.* **22**, 389–428.